Lithos 151 (2012) 57–73

Contents lists available at SciVerse ScienceDirect

Lithos

journal homepage: www.elsevier.com/locate/lithos

Geochemistry, geochronology, and origin of the Neoarchean Planalto Granite suite, Carajás, Amazonian craton: A-type or hydrated charnockitic granites?

G.R.L. Feio [a,b,e,*], R. Dall'Agnol [a,b], E.L. Dantas [c], M.J.B. Macambira [b,d], A.C.B. Gomes [a], A.S. Sardinha [a], D.C. Oliveira [a,b,e], R.D. Santos [a,b], P.A. Santos [a,b]

[a] Grupo de Pesquisa Petrologia de Granitóides, Instituto de Geociências (IG), Universidade Federal do Pará (UFPA), Rua Augusto Corrêa, 01. CEP 66075-110. Brazil
[b] Programa de pós-graduação em Geologia e Geoquímica, IG — UFPA, Brazil
[c] Laboratório de Estudos Geocronológicos, Geodinâmicos e Ambientais, Universidade de Brasília, Brasília, DF, CEP 70910-900, Brazil
[d] Laboratório de Geologia Isotópica, IG — UFPA, Brazil
[e] Faculdade de Geologia, Campus de Marabá, UFPA, Brazil

ARTICLE INFO

Article history:
Received 21 February 2011
Accepted 28 February 2012
Available online 7 March 2012

Keywords:
A-type granite
Charnockitic rocks
Hydrated charnockite
Archean
Carajás
Amazonian craton

ABSTRACT

New whole-rock geochemistry and LA-MC-ICPMS and Pb-evaporation geochronological data were obtained on zircon from the Neoarchean Planalto suite granites and associated charnockitic rocks of the Canaã area of the Carajás province, eastern Amazonian craton, Brazil. The Pb-evaporation ages of three samples from the Planalto suite are around 2730 Ma (2733 ± 2 Ma, 2731 ± 1 Ma and 2736 ± 4 Ma), whereas U–Pb LA-MC-ICPMS concordia ages obtained for these samples are 2729 ± 17 Ma, 2710 ± 10 Ma, and 2706 ± 5 Ma, respectively. An orthopyroxene quartz gabbro associated with the Pium complex and Planalto suite yielded a U–Pb concordia age of 2735 ± 5 Ma, interpreted as its crystallization age. The Planalto suite granites and the charnockitic rocks associated with the Mesoarchean Pium complex were probably crystallized at 2730 ± 10 Ma. The Planalto granites have ferroan character and are similar geochemically to reduced A-type granites. In previous studies, they have been classified as such, despite the fact that they are syntectonic. The tectonic setting and the association between the Planalto suite and charnockitic series led us to classify these biotite–hornblende granites as hydrated granites of the charnockitic series. The Planalto suite and the Neoarchean charnockitic magmas were more probably derived by partial melting of mafic to intermediate tholeiitic orthopyroxene-bearing rocks similar to those of the Pium complex. At 2.76 Ga, upwelling of asthenospheric mantle in an extensional setting propitiated the formation of the Carajás basin. Later on, at ca. 2.73 Ga, heat input associated with underplate of mafic magma induced partial melting of mafic to intermediate lower crustal rocks, originating the Planalto and charnockitic magmas. The emplacement of these magmas occurred under active regional stress and resultant major shear zones found in the Canaã dos Carajás area. The close association between the Planalto suite and charnockitic rocks suggests that they are similar to the high temperature granite magmatism found near the borders of Precambrian domains with different ages and tectonic evolution or in their zone of interaction.

1. Introduction

A-type granites are a distinctive group of rocks of diversified magmatic origin (Anderson and Bender, 1989; Bonin, 2007; Collins et al., 1982; Dall'Agnol et al., 2005; Eby, 1992; Frost and Frost, 1997; Loiselle and Wones, 1979; Nardi and Bitencourt, 2009; Rämö and Haapala, 2005; Whalen et al., 1987). They are normally associated with anorogenic or post-collisional extensional tectonic settings (Sylvester, 1989; Whalen et al., 1987) and are generally undeformed. However, in southern Brazil, early post-collisional deformed granites interpreted as A-type granites derived of tholeiitic series have been described (Florisbal et al., 2009; Nardi and Bitencourt, 2009).

A-type granites are abundant in the late Paleoproterozoic and Mesoproterozoic, between 1900 and 1000 Ma, when most of the rapakivi granites and anorthosite–mangerite–charnockite–granite (AMCG) complexes were formed (Emslie, 1991; Rämö and Haapala, 1995). However, comparatively earlier Paleoproterozoic ~2.44 Ga A-type intrusions are found, e.g., in eastern Finland (Lauri et al., 2006); these are relatively enriched in the high-field-strength elements (HFSE) and show, in this respect, some affinity with A-type granites also described from Archean terranes (e.g., Yilgarn craton; Champion and Sheraton, 1997). Archean granites associated with rocks of the charnockitic series (nomenclature adopted in this paper for the hypersthene-bearing rocks of the charnockitic series follows that of Le Maitre et al., 2002, their Table 2.10) have also been

* Corresponding author at: Grupo de Pesquisa Petrologia de Granitóides, Instituto de Geociências (IG), Universidade Federal do Pará (UFPA), Rua Augusto Corrêa, 01. CEP 66075-110. Brazil.

0024-4937/$ – see front matter © 2012 Elsevier B.V. All rights reserved.
doi:10.1016/j.lithos.2012.02.020

identified in the Kaapvaal, Siberian, and Singhbhum-Orissa cratons and the East Antarctic shield (Larin et al., 2006; Misra et al., 2002; Moore et al., 1993; Sheraton and Black, 1988). In the Archean, granites with A-type affinity are generally restricted to the Neoarchean.

Neoarchean granite bodies with A-type affinity have also been described in the Carajás Province, Amazonian craton, Pará state, northern Brazil. They include the Estrela Complex and the Serra do Rabo and Igarapé Gelado plutons (Barros et al., 2009; Sardinha et al., 2006) within or northwest of the Carajás basin (Fig. 1). Moreover, immediately to the south of the Carajás basin, several elongated plutons with A-type characteristics have been reported and are grouped in the present paper in the Planalto Suite. This suite is spatially associated with charnockite rocks and peculiar sodic granitoids and is found only in the Carajás basin. 1.88–1.87 Ga post-kinematic (yet synorogenic) granitoids with A-type and C-type granite characteristics related to a bimodal (mafic–felsic) magmatic association were also identified in the Central Finland Granitoid Complex (Elliott, 2003; Rämö et al., 2001).

In this paper, we present geological, geochemical, geochronological, and Nd isotope data for the Archean granites of the Planalto suite of the Carajás Province. The new data are employed to discuss the petrogenesis of this Neoarchean granitoid magmatism, the complex relationships between A-type granites and charnockitic series, and implications for crustal evolution of the northern Carajás Province.

2. Tectonical setting and regional geology

The Archean Carajás Province of the Amazonian craton comprises two distinct tectonic domains (Fig. 1a, b; Santos et al., 2000; Tassinari and Macambira, 2004; Vasquez et al., 2008): The Mesoarchean Rio Maria domain (RMD) in the south (3.0 to 2.86 Ga; Almeida et al., 2011; Leite et al., 2004; Macambira and Lancelot, 1996; Souza et al., 2001) and the Carajás domain in the north (3.0 to 2.55 Ga; Dall'Agnol et al., 2006; Gibbs et al., 1986; Machado et al., 1991). The border zone between the RMD and the Carajás domain is located north of the Sapucaia belt (Fig. 1b).

The Mesoarchean Rio Maria domain (Fig. 2) is composed of greenstone belts (3.00–2.90 Ga; Macambira, 1992; Souza et al., 2001) and several granitoid series: (1) Older tonalite–trondhjemite–granodiorite (TTG) series with four distinct units (2.98–2.93 Ga; Almeida et al., 2011; Althoff et al., 2000; Leite et al., 2004; Macambira and Lancelot, 1996); (2) Rio Maria sanukitoid suite (~2.87 Ga; Macambira and Lancelot, 1996; Oliveira et al., 2009); (3) Younger TTG series (~2.87–2.86 Ga; Almeida et al., 2011; Leite et al., 2004); (4) High Ba–Sr leucogranodiorite–granite suite (~2.87 Ga; Almeida et al., 2010); and (5) Potassic leucogranites of calc-alkaline affinity (~2.87–2.86 Ga; Leite et al., 2004).

The northern part of the Carajás domain (Fig. 2) corresponds to the Neoarchean Carajás basin (CB). Its southern part was denominated informally as 'Transition subdomain', a terrane originally similar to the RMD but intensely affected by the magmatic and tectonic Neoarchean events recorded in the CB (Dall'Agnol et al., 2006 and references therein; Domingos, 2009). However, Feio (2011) argued that the crustal evolution of the Canaã area and possibly also that of the Transition subdomain is distinct from the evolution of the RMD, and suggested that the Canaã area could belong to another tectonic terrane.

The Transition subdomain comprises poorly known, strongly deformed Mesoarchean to Neoarchean granitoid and gneissic rocks generally grouped in the Xingu Complex (Fig. 1b). In the Canaã area (Figs. 1c, 2), studied in more detail, four major magmatic events, three Mesoarchean and one Neoarchean, were distinguished (Feio,

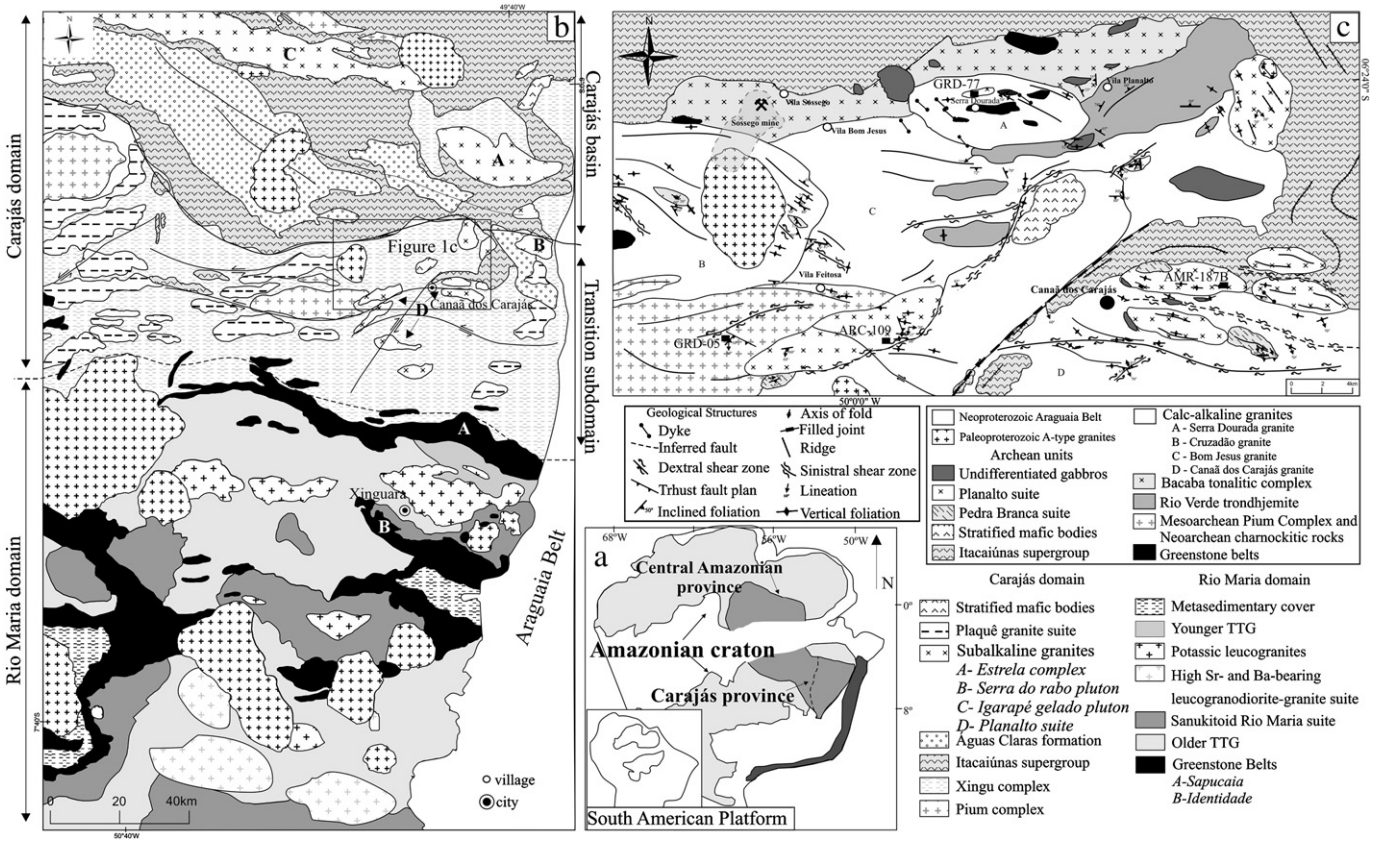

Fig. 1. (a) Location of the Carajás Province in the Amazonian craton. (b) Geological map of the Carajás Province, showing the location of the Canaã dos Carajás area and the approximate limits between the Rio Maria and Carajás domains (dashed line), and the Carajás basin and transitional subdomain (continuous lines). (c) Geological map of the Canaã dos Carajás area, showing the location of the dated samples.

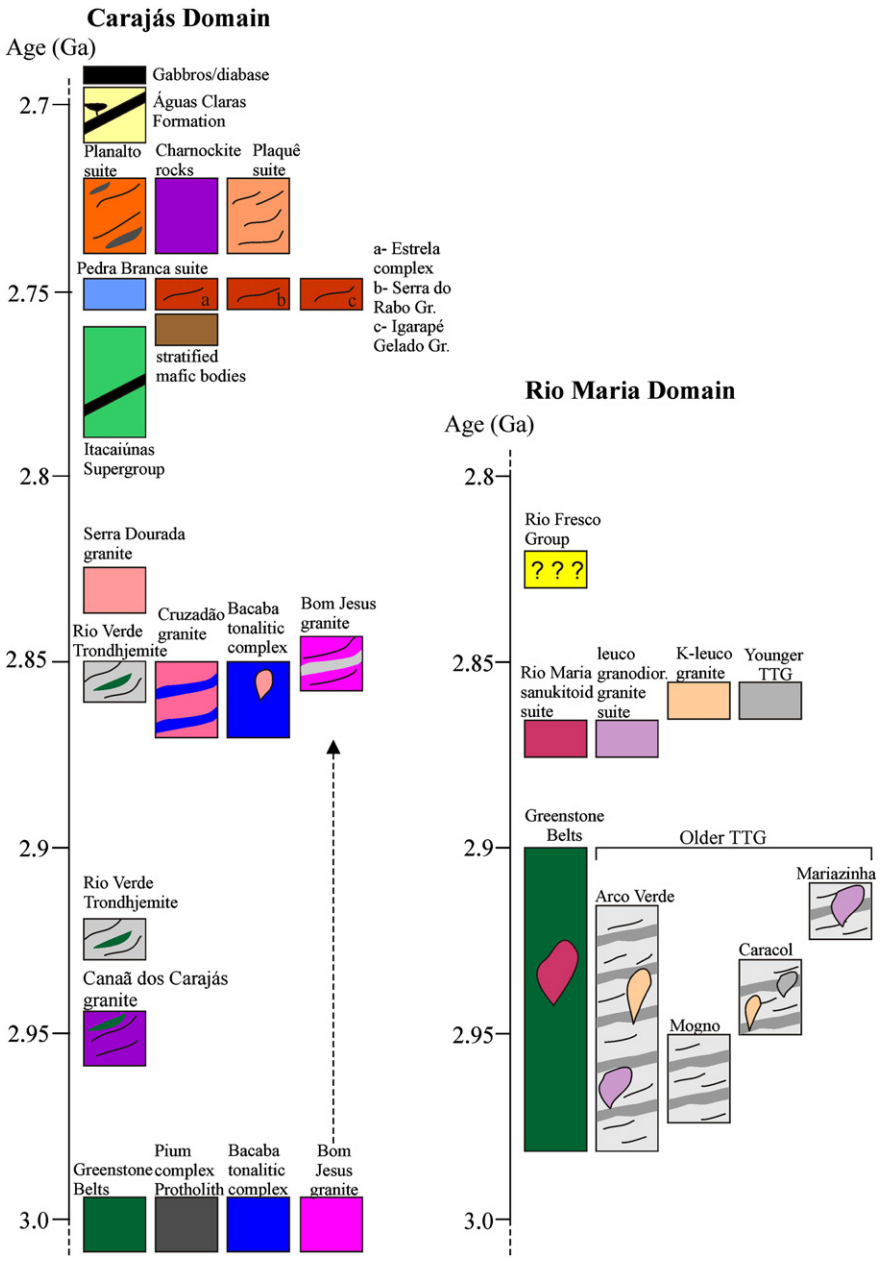

Fig. 2. Chronostratigraphic diagram of the northern part of the Carajás domain and Rio Maria domain (Carajás province of the Amazonian craton, Brazil).

2011): (1) 3.05–3.0 Ga protoliths of the Pium complex, the older rocks associated with the Bacaba tonalitic complex (Moreto et al., 2011) and possibly other rocks, as indicated by the common occurrence of inherited zircons with similar ages in younger rocks; (2) 2.96–2.93 Ga Canaã dos Carajás granite and the older rocks of the Rio Verde trondhjemite; (3) 2.87–2.83 Ga diversified granitoids in the Bacaba tonalitic complex, Rio Verde trondhjemite, and the Cruzadão, Bom Jesus and Serra Dourada granites; and (4) 2.75–2.73 Ga Planalto granite suite, accompanied by minor stocks of the Pedra Branca suite and charnockitic rocks.

The Neoarchean Carajás basin (Fig. 2) consists of banded iron formations, bimodal volcanic rocks (Itacaiúnas Supergroup, Gibbs et al., 1986; 2.76–2.74 Ga), metamorphosed in greenschist conditions, and siliciclastic (fluvial to marine) metasedimentary rocks of the Águas Claras formation (Nogueira et al., 1995). In the borders of the Carajás basin there are also several Neoarchean mafic–ultramafic stratified bodies (e.g., Vermelho in the Canaã area; Vasquez et al., 2008 and references therein), mineralized in nickel. Sills and dykes of Neoarchean gabbros cross-cut all these rocks. Stocks of Paleoproterozoic (1.88 Ga) A-type anorogenic granites, e.g., the Rio Branco pluton west of the Canaã area (Fig. 1c), locally intrude the Archean units.

The three Mesoarchean events identified in the Canaã area (Feio, 2011) comply with those of the Carajás province as a whole. However, the Neoarchean event is present only in the Carajás domain, where it is marked by widespread plutonic magmatism (Figs. 1c, 2): (1) Charnockitic rocks, quartz norites to enderbites (Pb-evaporation zircon age 2754 ± 1 Ma; Gabriel et al., 2010), closely associated with the Pium complex; (2) ~2.75 Ga sodic granitoids of the Pedra Branca suite (Gomes and Dall'Agnol, 2007), spatially associated with Planalto suite granites; and (3) Subalkaline granites in the Carajás basin (Figs. 1b, 2) — the Estrela complex (~2.76 Ga; Barros et al., 2009) and Serra do Rabo (2.74 Ga; Sardinha et al., 2006), Igarapé Gelado (2.73 Ga; Barros et al., 2009), and Old Salobo plutons (2.57 Ga; Machado et al., 1991).

The origin and evolution of the Carajás basin is still controversial — both continental rift (Dall'Agnol et al., 2006; Domingos, 2009; Gibbs et

al., 1986; Macambira, 2003; Nogueira et al., 1995) and continental margin (Barros et al., 2009; Lobato et al., 2006; Teixeira and Eggler, 1994) settings have been proposed. However, the Itacaiúnas supergroup metavolcanic sequences were formed dominantly by bimodal magmatism and abundant TTG or calc-alkaline series are absent in the Neoarchean, which is more consistent with a rift setting (Dall'Agnol et al., 2006). Nd isotope data on the Paleoproterozoic Serra dos Carajás suite further indicates the existence of a Mesoarchean substratum in the Carajás region similar isotopically to that of the RMD (Dall'Agnol et al., 2005; Tassinari and Macambira, 2004). Hence, a rift tectonic setting is more probable for the Carajás basin. Domingos (2009) concluded that tectonic inversion of the Carajás basin involved a regional phase of sinistral transpression controlled by a general NNE-directed oblique shortening.

3. Geological features of the Planalto suite and associated units

3.1. Pium complex and associated charnockitic rocks

The Pium complex is restricted to the Transition subdomain and was described as an orthopyroxene-bearing felsic to mafic granulitic complex (Araújo and Maia, 1991). It comprises three elongate bodies, with maximum length of 35 km, parallel to regional E–W foliation. In the type area, the Pium complex is composed dominantly of norite and gabbro with subordinate quartz- and orthopyroxene-bearing rocks modified by ductile deformation and recrystallization (Ricci and Carvalho, 2006; Santos and Oliveira, 2010). Field relationships between the mafic rocks and quartz gabbros, enderbites and charnockites indicate that the mafic rocks are found as partially digested enclaves (Araújo and Maia, 1991) or angular fragments (Santos and Oliveira, 2010) in the quartz–orthopyroxene-bearing rocks. These features suggest that the norite and gabbros were emplaced earlier and may be significantly older than the quartz–orthopyroxene-bearing rocks.

Pidgeon et al. (2000) dated an enderbite of the Pium complex by SHRIMP U–Pb on zircon at 3002 ± 14 Ma (protolith age from zircon cores) and 2859 ± 9 Ma (age of granulite facies metamorphism from rims). However, the metamorphic character of the Pium complex and the significance of the ages obtained by Pidgeon et al. (2000) were challenged and an igneous origin for the orthopyroxene-bearing rocks was proposed (Ricci and Carvalho, 2006; Santos and Oliveira, 2010; Vasquez et al., 2008).

3.2. Pedra Branca suite

The Pedra Branca suite consists of small stocks spatially associated with the plutons of the Planalto Suite (Fig. 1c). Field relationships between the Pedra Branca suite and the Planalto suite and other older Archean units were not observed. The suite is composed of strongly deformed sodic granitoids (tonalite and trondhjemite), with hornblende and biotite as the main mafic minerals, titanite, allanite, zircon, and apatite as accessory minerals, and, locally, relics of clinopyroxene (Gomes and Dall'Agnol, 2007).

The rocks of the Pedra Branca suite commonly alternating decimeter- to meter-thick tonalitic and trondhjemitic bands and subvertical E–W foliation related to ductile deformation. Additionally, in a stock located in the southeastern part of the mapped area (Fig. 1c), a thrust fault intercepts primary foliation and implies a later N–S compressive strain (Gomes and Dall'Agnol, 2007).

Geochronological data for a trondhjemite sample (AMR-191A) of the Pedra Branca suite yielded ages of 2749 ± 6 Ma and 2765 ± 39 Ma (Pb-evaporation and U–Pb TIMS ages on zircon, respectively; Sardinha et al., 2004). A further sample of trondhjemite (AMR-121E) yielded a U–Pb (TIMS) upper intercept age of 2737 ± 3 Ma. Feio (2011) dated a sample of this granitoid unit by U–Pb LA-MC-ICPMS on zircon and obtained a concordia age of 2750 ± 5 Ma (MSWD = 3.9) with 2954 ± 52 Ma inherited zircons and considered a crystallization age of ca. 2750 Ma for that granitoid.

3.3. Planalto suite

The Planalto suite consists of several E–W elongated lenticular granite plutons of less than 10 km in the largest dimension (Fig. 1c), generally bounded by shear zones and oriented concordantly to the dominant EW-trending regional structures. These plutons are intrusive in the Mesoarchean granitoid units, the mafic Pium complex, and the Neoarchean supracrustal Itacaiúnas supergroup (Fig. 1c), and they are spatially associated with the mafic rocks of the Pium complex, the charnockitic rocks and the Pedra Branca suite. The Planalto granite includes angular and partially digested enclaves of Pium mafic rocks (Fig. 3a, b, c, d). The Planalto and Pedra Branca granitoids show similar deformational features. These units and the charnockitic rocks were affected by high-angle thrust faulting.

The Planalto granites show penetrative subvertical E–W foliation sometimes accompanied by a remarkable high-angle stretching mineral lineation and C-type shear bands. True mylonites are found in sinistral (or subordinate dextral) shear zones. The less-deformed rocks exhibit well-preserved magmatic textures. The granites are cut by decimeter- to meter-thick pegmatoid veins and by narrow aplitic and microgranite dikes. Besides the Pium mafic xenoliths (Fig. 3a, b, c, d), the Planalto granite includes oval-shaped or quadratic enclaves of originally mafic or intermediate rocks that are now crowded with alkali-feldspar megacrysts incorporated from the granite magma (Fig. 3e, f); these enclaves are interpreted as evidence of local coexistence and mingling of the granite magma with a more mafic magma.

The Planalto suite is composed of monzogranite to syenogranite with varying contents of hornblende and biotite. The primary accessory minerals are zircon, apatite, allanite, and ilmenite ± fluorite. Relics of clinopyroxene included in amphibole are observed in some samples. Secondary minerals are epidote, muscovite, and chlorite ± scapolite ± carbonate ± titanite ± magnetite ± tourmaline.

The less-deformed granites of the suite are pink to reddish, predominantly coarse- or medium-grained equigranular to porphyritic with euhedral alkali feldspar phenocrysts in a medium- to fine-grained matrix. Plagioclase (An_{25-17}), locally altered and mantled by alkali feldspar (Fig. 4a), is present in the porphyritic varieties. In a small, possibly epizonal body, quartz and alkali feldspar form granophyric intergrowths surrounding euhedral plagioclase, and biotite is found as aggregates of euhedral crystals.

Most rocks display porphyroclasts of quartz, perthitic alkali-feldspar, and plagioclase, showing core-and-mantle microstructures. The quartz is also found as ribbons and recrystallized aggregates (Fig. 4b). Plagioclase shows deformed twinning and local recrystallization to fine-grained polygonal aggregates of largely untwinned grains. Bulbous myrmekite is common, replacing the borders of alkali-feldspar grains. Amphibole is present as medium-grained oval porphyroclasts (Fig. 4c) or forms oriented aggregates together with biotite and other mafic minerals. In the mylonites, foliation is deflected around alkali-feldspar porphyroclasts and strain shadows are marked by fine-grained recrystallized aggregates (Fig. 4d).

4. Elemental geochemistry

4.1. Pium complex charnockites and associated rocks

The Pium complex charnockites and associated norites, quartz–gabbro, and enderbites display subalkaline tholeiitic geochemical affinity (Santos, 2009). According to Santos (2009), the noritic varieties have SiO_2 contents varying from 51 to 55 wt.%, moderate Al_2O_3 (14.4 to 15.9 wt.%), Mg# (0.44 to 0.56), and Ba, high CaO (7.1 to 10.0 wt.%), FeOt (8.2 to 11.1 wt.%), Sr, and Zr, and low Nb and Rb. The quartz gabbro and enderbite show SiO_2 contents between (57.2 to 63.7 wt.%),

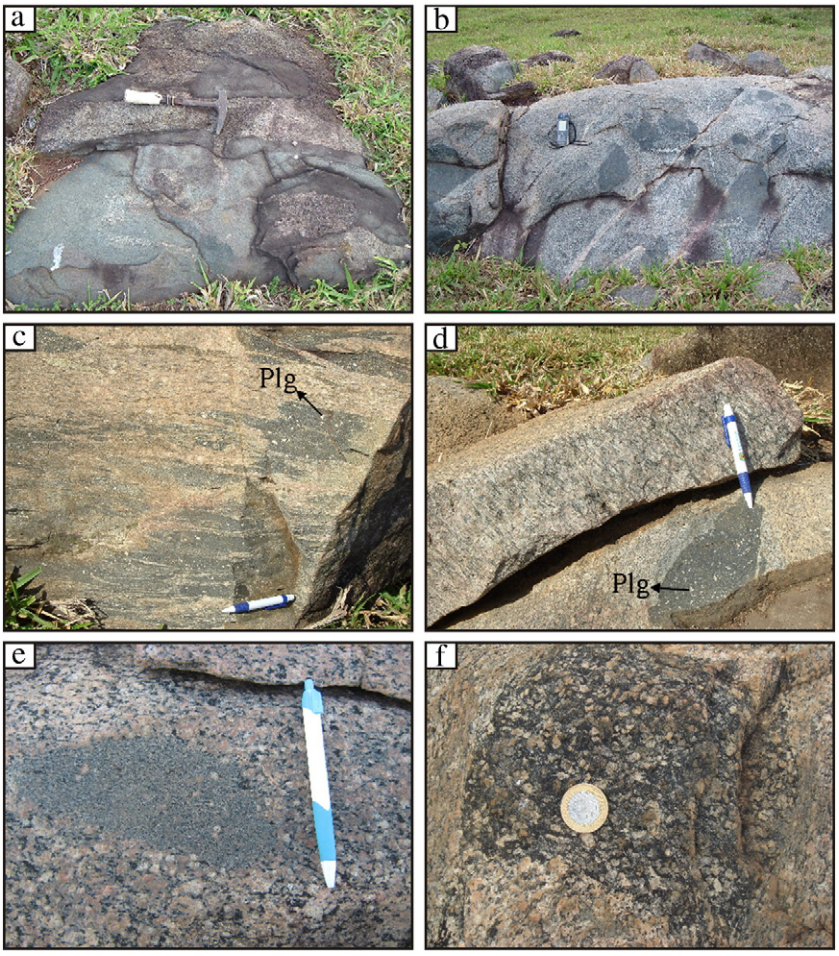

Fig. 3. Field aspects of the Planalto suite rocks (a, b, c, d). Angular, partially digested enclaves of Pium mafic rocks in the Planalto granite. In c and d, amphibolitic rocks composed of plagioclase phenocrysts in a fine-grained matrix of amphibole and epidote which are found in the contact between the Planalto granite and the mafic rocks of the Pium complex. In e and f, oval- or quadratic-shaped enclaves of mafic or intermediate rocks were included in the Planalto granite, with alkali-feldspar xenocrysts from the granite.

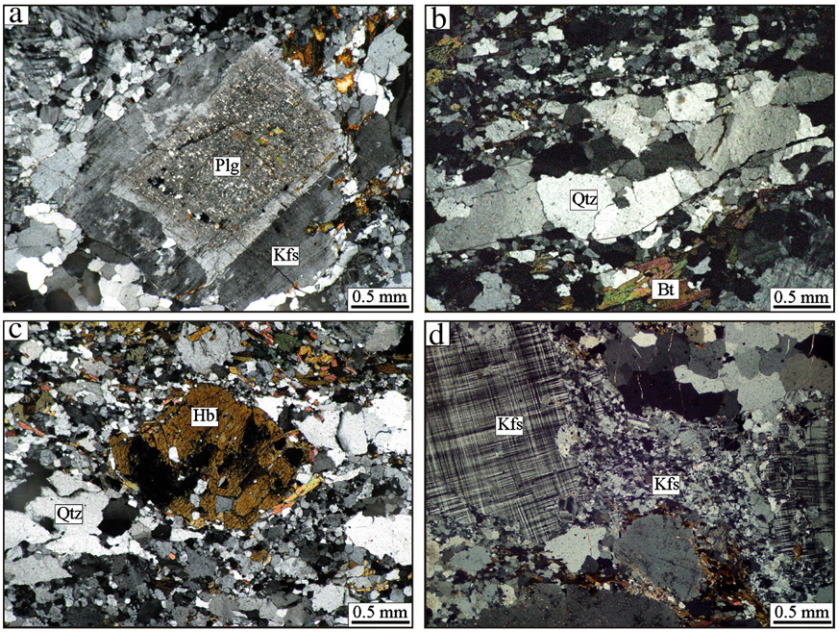

Fig. 4. Photomicrographs of the Planalto granite. (a) Plagioclase mantled by alkali feldspar. (b) Recrystallized aggregates of quartz. (c) Oval porphyroclast of amphibole with tails of recrystallized quartz in a mylonitized granite. (d) Alkali feldspar porphyroclasts showing strain shadows formed by the fine-grained recrystallized aggregates. Mineral abbreviations according to Kretz (1983).

Table 1
Representative chemical compositions of the granites of the Planalto suite of the Canaã dos Carajás area.

Unit	Planalto suite																				Charnockite
Sample	AMR-152	ARC-147	ARC-144	ARC-109	AMR-209	AMR-137A	AMR-187B	AMR-85A	AMR-149	AER-72A	AMR-140	AC-4B	AMR-145	ARC-77	ARF-17	AMR-116	AMR-208A	ARC-104	AMR-171	AMR-177	GRD-05
Varieties	BHMzG	BHMzG	BHMzG	HBSG	BHMzG	BHSG	HSG	HSG	HBMzG	BMzG	BHMzG	BHSG	BHSG	BSG	HBSG	BHSG	BSG	BMzG	BSG	HAG	Opx-Qtz gabbro
SiO_2	70.39	71.35	71.41	71.66	71.80	72.80	72.91	73.25	73.28	73.35	73.44	73.44	73.45	73.80	73.84	74.13	74.17	74.86	75.51	75.62	57.19
TiO_2	0.64	0.38	0.52	0.44	0.28	0.38	0.31	0.29	0.41	0.28	0.32	0.35	0.42	0.29	0.30	0.25	0.23	0.20	0.15	0.14	1.85
Al_2O_3	12.32	13.44	12.61	12.77	12.51	12.48	11.67	12.47	11.13	13.13	12.52	12.34	11.69	12.25	11.96	12.21	11.67	11.41	11.63	12.01	13.04
Fe_2O_3t	5.42	3.50	4.35	4.21	5.07	4.25	4.80	3.87	4.67	2.42	3.27	3.65	4.69	3.64	3.71	3.79	4.60	2.49	2.80	2.39	12.70
MnO	0.07	0.04	0.04	0.03	0.04	0.05	0.05	0.02	0.05	0.02	0.04	0.04	0.07	0.02	0.04	0.05	0.02	0.02	0.02	0.02	0.12
MgO	0.58	0.32	0.46	0.36	0.12	0.21	0.10	0.10	0.25	0.29	0.23	0.28	0.25	0.26	0.17	0.11	0.03	0.12	0.12	0.03	2.51
CaO	2.18	1.74	2.15	1.71	1.21	1.53	1.67	1.30	1.46	1.25	1.32	1.37	1.37	0.63	1.16	1.36	0.71	0.99	0.48	0.43	5.84
Na_2O	3.16	3.55	3.20	3.25	2.92	3.25	2.99	3.58	2.95	3.47	3.26	3.32	2.88	2.79	3.04	3.17	2.36	2.51	2.36	3.42	3.41
K_2O	3.93	4.55	4.01	4.49	5.20	4.04	4.44	4.21	3.49	4.71	4.45	4.14	3.83	5.11	4.75	4.65	5.36	5.03	5.64	5.09	2.36
P_2O_5	0.13	0.09	0.10	0.09	0.04	0.04	0.04	0.04	0.05	0.06	0.04	0.07	0.08	0.03	0.04	0.03	0.01	0.02	0.02	<0.01	0.51
LOI	0.80	0.70	0.80	0.70	0.50	0.60	0.70	0.30	1.60	0.80	0.50	0.80	0.70	1.00	0.60	0.00	0.50	2.10	1.00	0.70	0.20
Total	99.62	99.66	99.65	99.71	99.69	99.63	99.68	99.43	99.34	99.78	99.39	99.80	99.43	99.82	99.61	99.75	99.66	99.75	99.73	99.85	99.73
Ba	1624	1914	1842	1627	1722	1814	1459	4626	1765	1099	1142	1150	1929	949	1589	1391	1777	1488	1344	499	1038.0
Rb	97	94	101	117	132	120	102	71	85	123	158	150	83	127	127	134	94	124	112	67	52.2
Sr	204	167	169	145	88	173	103	92	161	85	137	141	153	58	101	96	103	88	76	36	239.5
Zr	595	356	465	487	399	502	504	499	462	283	387	396	543	355	432	393	596	303	295	316	293.6
Nb	26	15	19	21	22	24	21	7	19	13	24	22	19	24	26	16	24	24	29	11	19.2
Y	56	27	32	48	55	55	66	16	35	29	50	46	44	53	72	42	60	45	96	26	42.2
Hf	18	9	11	13	10	14	14	10	12	7	12	12	15	10	12	11	19	9	11	9	7.6
Ta	5	1	1	1	1	7	1	0	6	2	8	8	6	1	2	1	2	2	2	1	1.2
Th	10	15	22	24	14	14	23	5	11	19	27	21	11	32	44	12	23	19	31	14	14.1
U	2	4	5	4	6	4	3	1	3	5	6	5	2	5	7	2	6	6	12	3	3.2
Ga	23	18	17	18	20	22	20	16	19	17	21	20	18	18	18	20	21	17	22	17	19.8
La	81.7	28.4	43.1	64.4	43.1	84.4	130.0	29.2	56.7	59.3	99.0	102.2	68.3	100.2	118.4	63.0	59.3	68.0	143.7	78.0	57.30
Ce	179.6	78.6	87.0	130.4	97.6	162.7	249.7	58.8	107.6	124.7	203.0	206.7	137.6	197.2	237.3	130.5	124.1	133.5	263.3	148.7	125.70
Pr	19.5	7.5	10.9	16.3	12.3	17.2	26.5	7.0	11.2	13.6	20.0	21.1	15.4	22.2	27.3	15.6	15.8	16.4	34.1	17.0	15.52
Nd	77.4	29.4	43.2	62.5	51.5	62.8	99.6	28.0	42.3	49.3	74.1	73.5	60.9	82.3	101.1	63.5	63.7	61.5	132.2	63.0	63.60
Sm	13.8	5.8	8.1	10.6	10.1	11.6	15.7	4.8	8.7	7.8	12.1	12.7	10.7	13.7	15.2	10.7	13.3	10.4	23.3	8.9	11.32
Eu	2.4	1.6	2.2	1.8	2.2	2.5	2.7	2.7	2.1	1.1	1.8	1.8	2.6	1.4	1.9	2.1	1.9	1.6	2.3	1.1	2.61
Gd	10.8	5.2	6.9	8.9	10.0	9.8	12.7	3.8	7.0	5.9	9.3	9.2	8.4	11.3	12.2	9.1	12.5	8.9	20.7	6.6	9.70
Tb	1.7	0.9	1.1	1.5	1.6	1.5	2.1	0.6	1.0	0.9	1.3	1.3	1.2	1.8	1.9	1.4	2.0	1.4	3.3	0.9	1.43
Dy	9.8	5.1	5.9	8.4	9.5	9.2	11.3	3.0	6.2	5.1	8.4	8.1	7.7	10.2	10.5	7.7	11.2	7.9	17.7	5.2	8.10
Ho	2.0	1.0	1.2	1.6	1.9	1.8	2.2	0.6	1.3	1.0	1.7	1.6	1.6	2.0	2.3	1.6	2.3	1.5	3.6	0.9	1.52
Er	5.6	2.9	3.3	4.7	5.4	5.3	6.8	1.9	3.7	2.9	4.9	4.5	4.5	5.5	6.9	4.5	6.5	4.4	10.1	2.9	4.26
Tm	0.9	0.5	0.5	0.7	0.8	0.8	1.0	0.3	0.5	0.4	0.7	0.7	0.6	0.8	1.1	0.6	1.0	0.7	1.6	0.4	0.62
Yb	5.2	3.0	3.1	4.6	5.5	4.8	6.6	1.9	3.7	2.9	4.4	4.2	4.0	5.1	6.9	4.4	6.4	4.3	9.1	2.9	3.96
Lu	0.7	0.4	0.5	0.7	0.8	0.7	1.0	0.3	0.5	0.4	0.6	0.6	0.6	0.8	1.1	0.7	1.0	0.6	1.5	0.4	0.58
FeOt/(FeOt + MgO)	0.89	0.91	0.89	0.91	0.97	0.95	0.98	0.97	0.94	0.88	0.93	0.92	0.94	0.93	0.95	0.97	0.99	0.95	0.95	0.99	0.82
K_2O/Na_2O	1.24	1.28	1.25	1.38	1.78	1.24	1.48	1.18	1.18	1.36	1.37	1.25	1.33	1.83	1.56	1.47	2.27	2.00	2.39	1.49	0.69
Eu/Eu*	0.58	0.85	0.86	0.56	0.65	0.68	0.56	1.88	0.81	0.47	0.50	0.48	0.81	0.32	0.41	0.63	0.45	0.51	0.31	0.41	0.74
(La/Yb)N	11.18	6.88	9.91	10.13	5.60	12.51	14.09	11.14	10.90	14.62	16.07	17.33	12.37	13.98	12.40	10.29	6.63	11.37	11.35	19.03	10.38
A/CNK	0.92	0.96	0.93	0.96	0.99	1.00	0.91	0.97	0.99	1.00	1.00	0.99	1.03	1.09	0.98	0.96	1.06	1.00	1.07	1.01	0.69

BHMzG — Biotite–hornblende monzogranite; HBSG — Hornblende–biotite syenogranite; BHSG — Biotite–hornblende syenogranite; HSG — Hornblende syenogranite; BMzG — Biotite monzogranite; BSG — Biotite syenogranite; HAG — Hornblende-biotite syenogranite; Opx — orthopyroxene; Qtz — quartz.

moderate Al_2O_3 (13.2 to 17.6 wt.%) and Mg# (0.25 to 0.56), and significantly higher K_2O, Ba, Zr, and Y, compared to the norite. The FeOt/(FeOt + MgO) ratios vary from 0.58 to 0.69 in the norite and from 0.68 to 0.84 in the quartz gabbro and enderbite, except for one anomalous value of 0.58. The heavy rare earth elements (HREE) show a flat normalized pattern and LREE enrichment is only moderate [$(La/Yb)_N$ generally between 5 and 14; Santos, 2009]. Most of the analyzed samples display discrete negative (or in rare cases positive) Eu anomalies (Eu/Eu* generally between 0.8 and 1.18).

The quartz gabbro analyzed in the present work (sample GRD-05; Table 1) has SiO_2 content of 57.19 wt.% and shows higher contents of TiO_2, FeOt, and K_2O, and lower of Al_2O_3 and MgO compared to rocks of the Pium complex with similar silica contents (cf. Santos, 2009). GRD-05 has a higher value of FeOt/(FeOt + MgO) (0.82) compared to Pium rocks (0.58 to 0.75), whereas trace element contents of GRD-05 are not significantly different from those of the Pium complex similar rocks.

4.2. Planalto suite

Representative chemical compositions of the Planalto suite are given in Table 1. The granites of the suite show a restricted range of silica (70.4 to 75.7 wt.%) and relatively high K_2O contents (generally between 4.0 and 5.5 wt.%). They have typically low Al_2O_3 (Fig. 5a; 11.1–12.8 wt.%), CaO (Fig. 5b; 0.4–2.2 wt.%) and MgO (Fig. 5c; 0.03–0.58 wt.%) contents. The K_2O/Na_2O (Fig. 5d; 1.2–2.3) ratios are high and the FeOt/(FeOt + MgO) ratios are above 0.88, corresponding to those of ferroan granites (Frost et al., 2001). A/CNK values vary from 0.91 to 1.09, indicating a mildly metaluminous to peraluminous character of these granites (Fig. 6a, Table 1). The Planalto suite granites have high contents of Zr (Fig. 5e), Y, Nb, and HREE and show geochemical affinity with reduced A-type granites (Fig. 6b, c; cf. Collins et al., 1982; Dall'Agnol and Oliveira, 2007; Eby, 1992; Whalen et al., 1987) and Archean alkaline granites (Fig. 6d; cf. Sylvester, 1989,

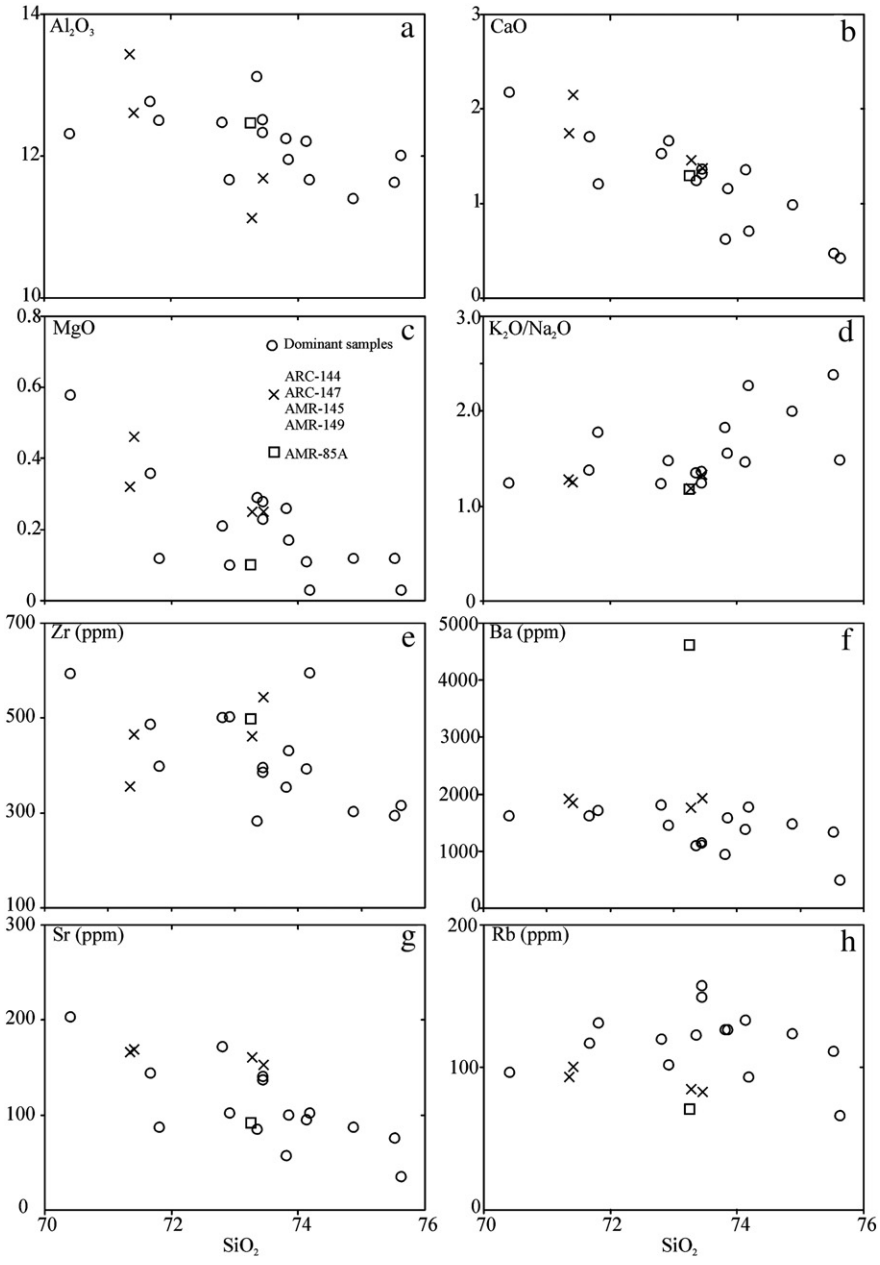

Fig. 5. Chemical composition of the Granites of the Planalto suite shown in SiO_2–Al_2O_3 (a), SiO_2–CaO (b), SiO_2–MgO (c), SiO_2–K_2O/Na_2O (d), SiO_2–Zr (e), SiO_2–Ba (f), SiO_2–Sr (g), and SiO_2–Rb (h) diagrams.

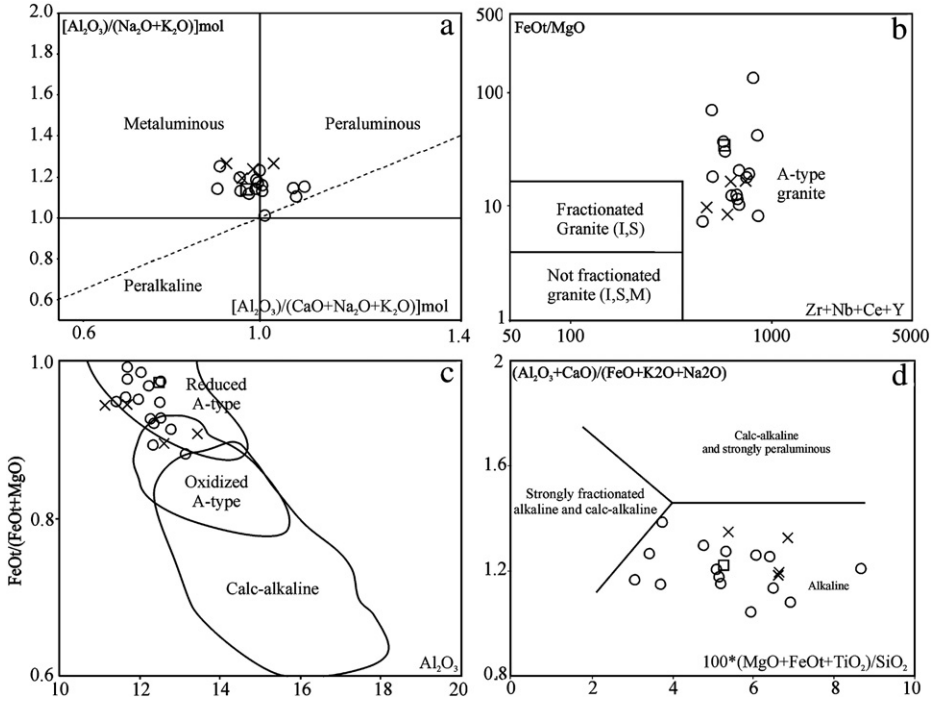

Fig. 6. Geochemical diagrams showing the composition of the samples of the Planalto suites of the Canaã dos Carajás area. (a) $[Al_2O_3/(CaO+Na_2O+K_2O)]$mol vs. $[Al_2O_3/(K_2O+Na_2O)]$mol diagram (Shand, 1950). (b) Zr + Nb + Ce + Y vs. FeO/MgO diagram of Whalen et al. (1987). (c) FeOt/(FeOt + MgO) vs. Al_2O_3 showing the compositional fields of calc-alkaline and A-type granites, and reduced and oxidized A-type granites (Dall'Agnol and Oliveira, 2007). (d) Major element discrimination diagram for leucogranites (Sylvester, 1989).

1994). They show high Ba (Fig. 5f; 949–1928 ppm), low to moderate Sr (Fig. 5g; 35–204 ppm), and low Rb (Fig. 5h; 67–158 ppm) contents.

REE patterns are similar for all analyzed samples with low $(La/Yb)_N$ ratios (5–19; Table 1), flat HREE segments (Fig. 7), and varying, mostly negative Eu anomalies ($Eu/Eu^* = 0.31–0.86$, Fig. 7a, b). The Eu and Sr behavior of dominant samples indicates fractionation of plagioclase during the magma differentiation or its retention in the magma source. Moreover, the flat REE pattern and the absence of concave-down curvature in the pattern of MREE to HREE suggests, respectively, that garnet and hornblende were not important fractionating phases.

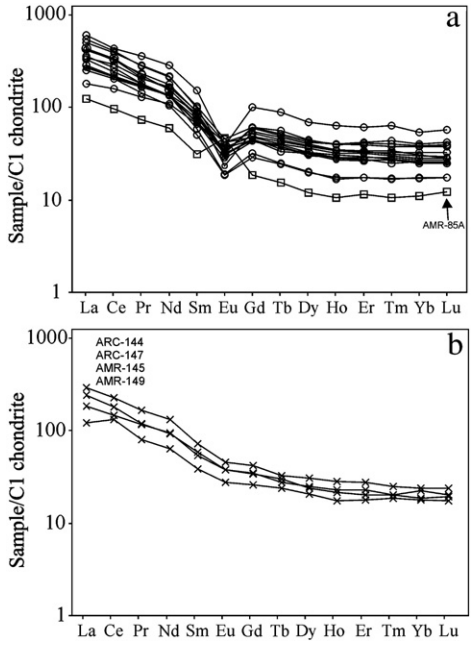

Fig. 7. REE patterns of the granites of the Planalto suite of the Canaã dos Carajás area: Values normalized to chondrite after Evensen et al. (1978). (a) Dominant patterns with negative Eu anomalies and an isolated sample with positive Eu anomaly. (b) Subordinate samples with no marked Eu anomaly.

5. Isotope geochemistry

The location of the four dated samples is shown in Fig. 1c and their geographical coordinates and analytical results are given in Table A (Supplementary Data). The dated samples come from two plutons and a small stock of the Planalto Suite and a local occurrence of a charnockitic rock in the principal domain of the Pium complex. The four dated rocks and two additional samples of the Planalto granite were analyzed for whole-rock Nd isotopes (Table 2).

5.1. Pb-evaporation and U–Pb LA-MC-ICPMS geochronology

5.1.1. Planalto suite

Hornblende syenogranite (AMR-187B) — For the Pb-evaporation method, 18 crystals were analyzed and six (Fig. 8a) were used to calculate a $^{207}Pb/^{206}Pb$ mean age of 2733 ± 2 Ma with a MSWD = 0.92. Analyses with high common Pb ($^{204}Pb/^{206}Pb > 0.0004$) scatter more than two standard deviations beyond the average age value, or less than five analyses in the block were discarded (these criteria were employed in all samples analyzed for the Pb-evaporation method). Two distinct populations of zircon (with cores and rims) were also analyzed by the U–Pb LA-MC-ICPMS method on zircon. The results indicate similar ages for the different populations and zones. In total, thirty-four zircon grains were analyzed and, after a critical assessment of the analytical results, ten spots yielded a discordant upper intercept age of 2713 ± 19 Ma (MSWD of 5.4; Fig. 9a) and five of them a concordia age of 2729 ± 17 Ma (MSWD of 1.7; Fig. 9a).

Hornblende-biotite syenogranite (ARC-109) — Eight zircon crystals were analyzed by the Pb-evaporation method, and six (Fig. 8b) of them were used to calculate a $^{207}Pb/^{206}Pb$ mean age of 2731 ± 1 Ma (MSWD = 2.0). The U–Pb LA-MC-ICPMS method was also employed for this sample and distinct cores and outer zones of the zircon crystals

Table 2
Sm–Nd isotopic data for the Planalto suite and orthopyroxene quartz gabbro of the Canaã dos Carajás area.

Sample	Sm (ppm)	Nd (ppm)	$^{147}Sm/^{144}Nd$	$^{143}Nd/^{144}Nd$ (±2σ)	f (Sm/Nd)	εNd (0)	εNd (t)	T_{DM} (Ma)
2.73 Ga Orthopyroxene quartz gabbro								
GRD-05	11.78	64.64	0.1102	0.51099(7)	−0.4398	−32.0	−1.6	3049
2.73 Ga Planalto suite								
ARC-108	6.02	42.00	0.0867	0.510573(9)	−0.5592	−40.3	−1.6	2996
ARC-109	11.35	63.00	0.1089	0.511013(7)	−0.4464	−31.7	−0.8	2988
AMR-152	13.82	77.83	0.1073	0.511098(12)	−0.4545	−30.0	+1.4	2813
AMR-187B	17.09	100.52	0.1027	0.510901(17)	−0.4779	−33.9	−0.9	2975
GRD-77	13.40	77.29	0.1048	0.510868(23)	−0.4672	−34.5	−2.3	3084

were analyzed (Fig. 9b). Fifteen selected analyses provided a concordia age of 2710 ± 10 Ma (MSWD of 8.1). Reducted separately, spots from cores and rims yielded consanguineous ages of 2716 ± 14 Ma (MSWD of 0.36) and 2703 ± 4 Ma (MSWD of 11.6), respectively.

Biotite syenogranite (GRD-77) — Six zircon crystals were analyzed by the Pb-evaporation method and yielded a $^{207}Pb/^{206}Pb$ mean age of 2736 ± 4 Ma with a MSWD of 3.0 (Fig. 8c). Twenty-seven zircon grains were analyzed by the LA-MC-ICPMS method and ten selected zircons define a discordia age of 2689 ± 23 Ma (MSWD of 5.1) and five define a concordia age of 2706 ± 5 Ma (MSWD of 3.9) (Fig. 9c).

The Pb-evaporation zircon ages obtained for the three samples of the Planalto granite are almost identical (2733 ± 2 Ma, 2731 ± 1 Ma, and 2736 ± 4 Ma). Similar ages were obtained by the U–Pb SHRIMP on zircon method for the samples AMR-187B and ARC-109 (2738 ± 3 Ma and 2730 ± 5 Ma, respectively; Feio, 2011). These ages are 10 to 20 Ma younger than those determined for other occurrences of the Planalto suite (2747 ± 2 Ma, Huhn et al., 1999) and by stocks in the southern part of the Transition subdomain (2754 ± 2 Ma, Silva et al., 2010; 2748 ± 2 Ma and 2749 ± 3 Ma, Souza et al., 2010). Other granites similar to the Planalto suite, the Estrela complex, the Igarapé Gelado and the Serra do Rabo plutons, yielded, respectively, zircon ages of 2763 ± 7 Ma and 2731 ± 26 Ma (Pb-evaporation; Barros et al., 2009) and 2743 ± 2 Ma (U–Pb TIMS age; Sardinha et al., 2006).

The ages obtained for the Planalto suite by the U–Pb LA-MC-ICPMS method show relatively larger variation. The samples AMR-187B, ARC-109 and GRD-77 gave, respectively, concordia ages of 2729 ± 17 Ma, 2710 ± 10 Ma, and 2706 ± 5 Ma. The core and outer zones of zircon grains do not show significant differences. The age of sample AMR-187B is superposed with those given by the Pb-evaporation method, whereas those of the two other dated samples are 10 to

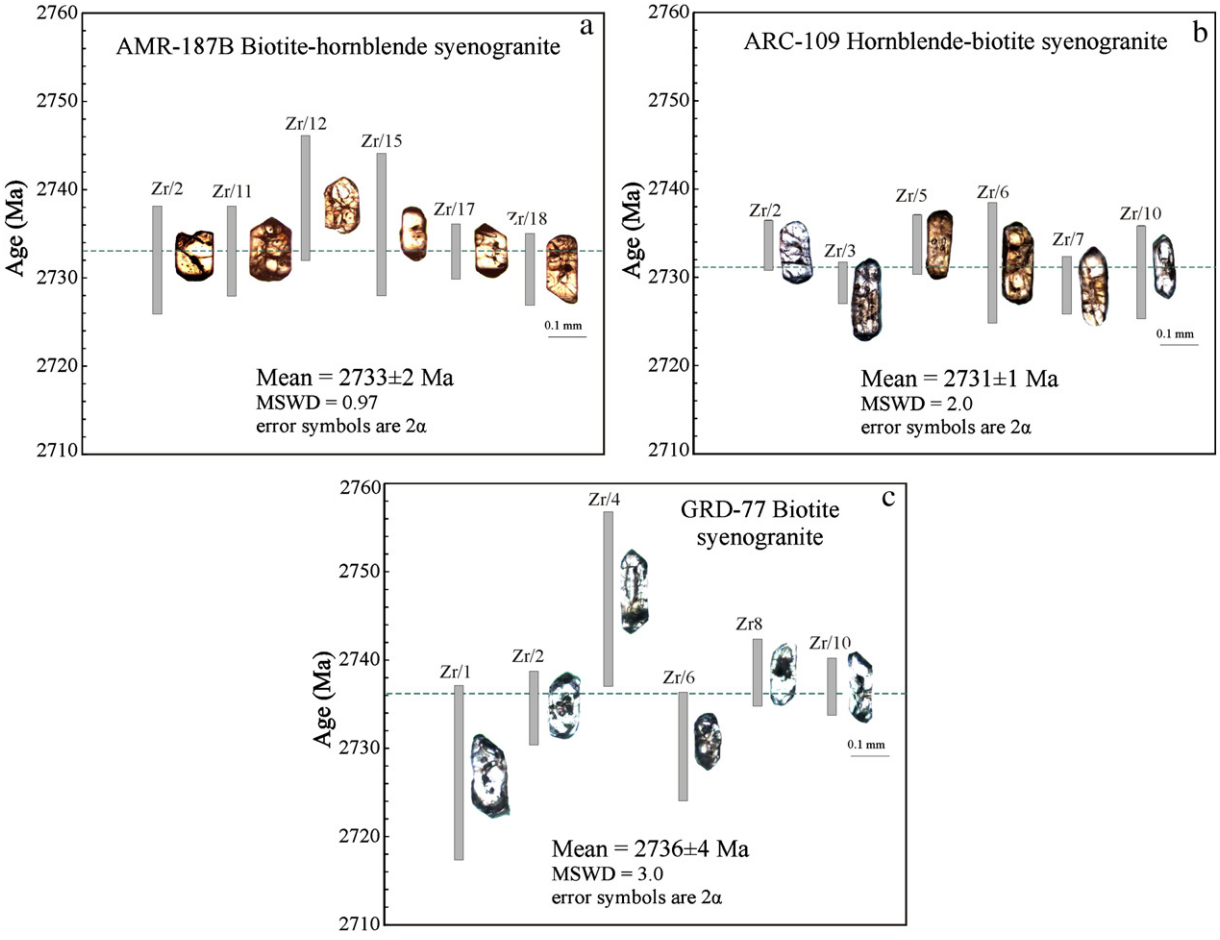

Fig. 8. Single zircon Pb-evaporation age diagrams for granites of the Planalto suite of the Canaã dos Carajás area: (a) Hornblende syenogranite (AMR-187B); (b) Hornblende–biotite syenogranite (ARC-109); and (c) Biotite syenogranite (GRD-77). Gray vertical bars represent the error for each determination and horizontal dashed lines correspond to the mean age of each sample. Images of the analyzed zircon grains are also shown.

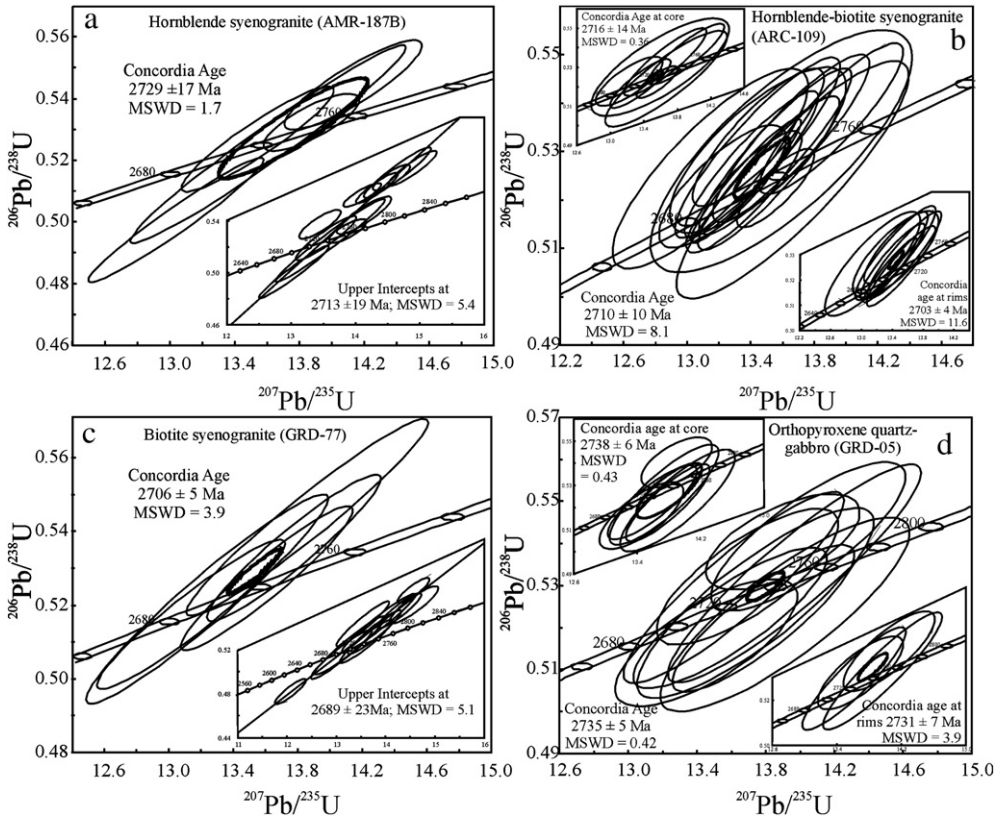

Fig. 9. LA-MC-ICPMS U–Pb concordia diagrams for the samples of the Planalto suite [(a) AMR-187B — a concordia age of five analyses and, in the inset, upper intercept age defined by ten spot analyses. (b) ARC-109 — concordia age of fifteen analyses from cores and rims and, in the insets, concordia ages by separate cores and rims. (c) GRD-77 — a concordia age of five analyses and, in the inset, upper intercept age for ten spot analyses] and orthopyroxene quartz gabbro [(d) GRD-05 — concordia age of thirteen analyses from cores and rims and, in the insets, concordia ages by separate cores and rims analyses].

20 Ma younger. The ages obtained by Pb-evaporation and U–Pb SHRIMP methods for samples AMR-187B and ARC-109 are superposed within errors and a similar age was also obtained on U–Pb LA-MC-ICPMS for sample AMR-187B. These results suggest that the Planalto suite granites were crystallized at 2730 ± 10 Ma.

5.1.2. Charnockitic rocks

The sample GRD-05 of the orthopyroxene quartz gabbro was selected for U–Pb LA-MC-ICPMS dating. 23 spot analyses were performed on different zircon grains and, whenever possible, both core and outer zones were analyzed. Thirteen analyses were discarded employing the criteria in Appendix B. The whole data indicate a concordia age (Fig. 9d) of 2735 ± 5 Ma (MSWD = 0.42). Reducted separately, cores and rims yielded concordia ages of 2738 ± 6 Ma (MSWD = 0.43) and 2731 ± 7 Ma (MSWD = 3.9). These data indicate no significant contrast in age between the cores and rims of the analyzed zircon crystals and we consider the age of 2735 ± 5 Ma as representative of the crystallization of the orthopyroxene quartz gabbro. This age is distinct from the ages assumed for the Pium complex (Pidgeon et al., 2000) and complies, within error, with the age yielded by the zircon crystals of the Planalto granite.

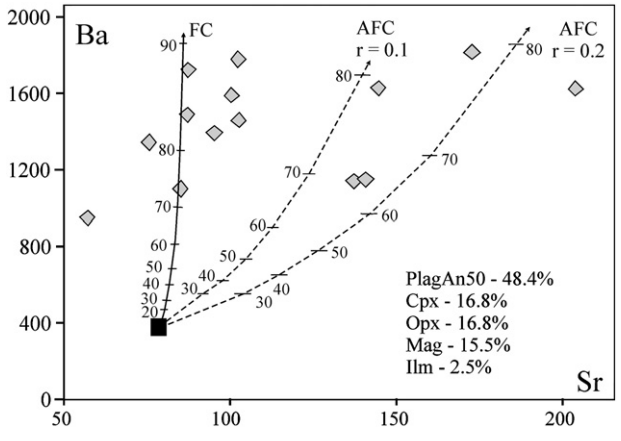

Fig. 10. Sr vs Ba variation diagram with FC and AFC trends for fractionating tholeiitic basalt (shown in increments of 10%). The AFC trends correspond to the assimilation of 10% or 20% of a mafic granulitic rock (CP-20, norite of the Pium complex; Santos, 2009). The initial basalt composition is that of a metabasalt of the Itacaiúnas supergroup (GB-82A; Gibbs et al., 1986). The lozenges indicate the composition of the Planalto granite samples.

5.2. Nd isotope data

The Sm and Nd values of the Planalto suite granites and the orthopyroxene quartz gabbro (6 to 17 ppm of Sm and 42 to 100 ppm of Nd; Table 2) are relatively high compared to those of other Archean granitoids of the Canaã area (1.2 to 4.9 of Sm and 10 to 31 of Nd; Feio, 2011). The $^{147}Sm/^{144}Nd$ ratios vary generally between 0.103 and 0.110 with the sample ARC-108 showing a lower value (Table 2). The Nd isotope data of the Planalto granites gave εNd(t) values varying from −0.8 to −2.2 and T_{DM} ages from 2975 to 3084 Ma (Table 2), except for the sample AMR-152 that shows εNd(t) of +1.4 and T_{DM} age of 2813 Ma. The GRD-05 sample of the orthopyroxene quartz gabbro yielded an εNd(t) value of −1.6 and a T_{DM} age of 3049 Ma (Table 2).

The initial Nd isotope composition of the Planalto suite samples and the charnockitic rock is rather similar (εNd values range from −2.3 to −0.8) as their T_{DM} model ages (2970 to 3080 Ma). These new Nd isotope results are largely superposed with those available

for the Estrela complex (Barros et al., 2009; their Table 7) which yielded εNd(t) values in the range from −2.1 to −0.4 and T_{DM} model ages of 2970 to 3190 Ma.

6. Discussion

6.1. Origin of the Planalto suite and associated rocks

To assess the origin and magmatic evolution of the Planalto granite and orthopyroxene quartz gabbro we performed major and trace element modeling using the software Genesis 4.0 (Teixeira, 2005). The chemical compositions and mineral-melt distribution coefficients applied for trace element modeling (Rollinson, 1993) are given as Supplementary Data (Tables B and C).

6.1.1. Planalto suite

Geochemical modeling was focused on the biotite–hornblende monzogranite (HBMzG) and the hornblende–biotite syenogranite (HBSG). These rocks are largely dominant in all studied plutons and were interpreted to represent initial magmatic liquids. Three hypotheses were considered to explain the origin of the Planalto granite magma: (1) derivation from a tholeiitic mafic magma by fractional crystallization (Florisbal et al., 2009; Frost and Frost, 1997; Nardi and Bitencourt, 2009) or from a mafic magma derived from an enriched-mantle source; (2) origin by combined assimilation-fractional crystallization involving a tholeiitic magma and undepleted granulitic mafic lower crust (cf. Elliott, 2003 and references therein) with a strong contamination by the older crust; and (3) partial melting of lower crustal undepleted 'granulitic' mafic rocks (Landenberger and Collins, 1996) or of Mesoarchean granitoids of the Canaã (protoliths separated from the mantle at ca. 3000 Ma).

6.1.1.1. Fractional crystallization (FC) of a basaltic magma. The ferroan and reduced character of the Planalto granites suggest that if a mafic magma was involved in their origin, it should be necessarily tholeiitic (Frost and Frost, 1997; Nardi and Bitencourt, 2009). The dominant tholeiitic magmas found in Archean terranes (Condie, 1993) have too low K_2O to be able to generate the Planalto magmas by fractional crystallization. Hence, we tested the hypothesis of a tholeiitic magma similar in composition to the Neoarchean metabasalts of the Itacaiúnas supergroup (Gibbs et al., 1986) as a possible source for the Planalto granite. The results imply a very large degree of fractionation (>80%) of plagioclase (An_{50}), clinopyroxene, orthopyroxene, magnetite, and ilmenite to derive the composition of the Planalto granite (cf. Fig. 10; Supplementary data, Table D).

6.1.1.2. Combined assimilation-fractional crystallization (AFC). A model involving the assimilation of a mafic lower crust by mantle-derived mafic magmas followed by fractional crystallization of the resulting magma (Elliott, 2003; Smithies et al., 2011) was also tested. We evaluated interaction of tholeiitic basalt magma that originated the metabasalts of the Itacaiúnas supergroup (Gibbs et al., 1986) and a norite of the Pium complex (Santos, 2009). A reasonable fit resulted by relatively low assimilation rates (r = 0.1 to 0.2) of the norite followed by ca. 80% of fractional crystallization of $plagioclase_{(An50)}$, clinopyroxene, orthopyroxene, magnetite, and ilmenite (Fig. 10; Supplementary Table D). The modeling suggests that AFC processes were also potentially able to form the Planalto magmas with relatively higher Sr contents compared to those obtained by FC only. Nevertheless, a large degree of magma fractionation was also necessary in the case of AFC processes.

6.1.1.3. Partial melting of lower crustal sources. The isotope data indicate that the Planalto magmas could have been derived by partial melting of older crustal rocks. Several models have been proposed to advocate a crustal source for A-type or similar granites: (1) melting of metaluminous diorite–tonalite–granodiorite sources (Anderson and Bender, 1989; Dall'Agnol et al., 2005; Patiño Douce, 1997); (2) varying degrees of partial melting of a dry granulite residue depleted by prior extraction of granitic melt (Clemens et al., 1986; Collins et al., 1982; Whalen et al., 1987); (3) partial melting of a dehydrated non-depleted mafic to intermediate 'charnockitized' lower crust with very low water activities and fO_2 and at high temperatures (>900 °C; Landenberger and Collins, 1996); and (4) partial melting of undepleted tholeiitic basalts and their differentiated equivalents (Frost and Frost, 1997).

The Mesoarchean granite suites identified in the Canaã area (Canaã dos Carajás, Bom Jesus, Cruzadão, and Serra Dourada granite) can be discarded as possible magma sources, because they show similar silica contents and are too evolved geochemically compared to the Planalto suite to be compatible with its source. A similar reasoning can be applied to the Rio Verde trondhjemite (2.93 to 2.85 Ga; Feio, 2011). The remainder potential sources exposed in the Canaã area are the diorite to granodiorite of the Bacaba complex (~2.85 Ga) and the Pium complex (Fig. 1c). The latter is closely linked with the Planalto suite and this makes more plausible a genetic relationship between them.

To verify possible sources for the Planalto magmas, a diorite and a tonalite sample (59.18 and 62.89 wt.% of SiO_2, respectively) of the Bacaba complex were tested and both samples gave very poor fit for major elements. Thus the origin of the Planalto magmas by partial melting of a source similar in composition to the rocks of the Bacaba complex is improbable.

To test the Pium complex rocks as a source for the Planalto magmas, we devised several equilibrium batch melting models. The results of the modeling are presented in Table 3 and the behavior of major element (Figs. 11a, 12a), LILE and HFSE (Figs. 11b, 12b) and REE (Figs. 11c, 12c) is depicted in Figs. 11 and 12 (only the results for AMR-152 are shown). The norite and associated quartz norite of the Pium Complex are both viable candidates for the source of the Planalto magmas. The melting of these rocks was able to generate liquids similar in composition to the hornblende–biotite syenogranite (ARC-109) and biotite–hornblende monzogranite (AMR-152) of the Planalto suite. In the case of the norite sample (Fig. 11a), the degree of melting was coincident and equal to 8% for both Planalto varieties and for the quartz norite it varied from 29 to 30% (Fig. 12a). The residual phases for the norite as a source were, in decreasing order of abundance, $plagioclase_{(An42)}$, clinopyroxene, orthopyroxene, magnetite, and ilmenite. The same residual phases, with similar proportions were obtained for the quartz norite (Table 3).

Geochemical modeling suggests that the Planalto suite could be derived by partial melting of mafic to intermediate tholeiitic orthopyroxene-bearing rocks similar to those of the Pium complex. This kind of source would more probably lead to reduced magmas (cf. Frost and Frost, 1997), which is consistent with the high FeOt/(FeOt + MgO) ratios of the Planalto Suite (>0.88; Table 3).

FC and AFC models are also apparently suitable to explain the origin of the Planalto magmas. However, they require a high rate of fractionation of the mafic basaltic magma that implies a low volume of granite liquids compared to the initial mafic magma. Furthermore, these models are apparently not able to explain the total dominance of monzogranites and syenogranites in the studied plutons of the Planalto suite and the lack of intermediate and less evolved granitoid rocks that could indicate the existence of an expanded magmatic series. It is concluded that these models are less suitable to explain the origin of the Planalto granites (Elliott, 2003, arrived at a similar conclusion regarding the origin of C- and A-type Paleoproterozoic granites of the Central Finland Granitic Complex) and the partial melting of undepleted mafic lower crust is our preferred model.

6.1.1.4. Differentiation of the Planalto magma. Possible factors controlling the differentiation of the Planalto magmas were also evaluated

Table 3
Geochemical modeling data for the granitoids of the Canaã dos Carajás area.

Original composition						(Co = CP-20)[1]		(Co = CP-42)[2]		(Co = CP-20)[3]
Samples	CP-20*	CP-42*	GRD-05	ARC-109	AMR-152	ARC109	AMR-152	ARC109	AMR-152	GRD-05
Lithologies	Norite	Qtz Norite	Qtz gabbro	HBSG	BHMzG	PM	PM	PM	PM	PM
SiO_2	50.92	54.96	57.19	72.51	70.39	71.58	71.21	73.15	70.99	57.54
TiO_2	1.33	1.38	1.85	0.32	0.64	0.22	0.3	0.52	0.67	1.78
Al_2O_3	15.42	14.39	13.04	13.81	12.32	12.76	12.13	12.86	12.51	13.08
Fe_2O_3	12.32	11.34	12.7	4.03	5.42	4.24	5.11	4.15	5.71	12.85
MgO	6.24	4.51	2.51	0.33	0.58	0.43	0.37	0.25	0.68	2.65
CaO	8.56	7.16	5.84	1.68	2.18	1.8	1.95	1.577	2.32	5.86
Na_2O	3.51	3.47	3.41	2.64	3.16	3.59	3.56	3.4	3.28	3.55
K_2O	0.73	1.36	2.36	5.31	3.93	5.38	5.36	4.1	3.84	2.68
Rb	14.9	26.9	52.2	114	97.1	119	119	77.21	65.19	71.32
Sr	318	340	239.5	269	203.9	305	304	328	331	303
Ba	423	772	1038	2119	1624.3	2053	2050	2040	1762	1485
Zr	124.2	164.8	293.6	374	594.5	680	682	446	380	445
Y	22.3	27.6	42.2	88.25	56.4	79.63	80.06	63.88	56.65	60.66
Nb	7.2	9.6	19.2	37.19	25.6	43.85	43.97	32.13	26.17	27.6
La	24	36.8	57.3	119	81.7	110	110	120	98.01	124
Ce	53.3	80.3	125.7	199	179.6	251	252	208	179	181
Nd	25.1	36.3	63.6	98.39	77.4	111	112	89.04	77.33	84.03
Sm	4.87	6.52	11.32	15.58	13.8	16.72	16.79	14.54	12.85	13.92
Eu	1.4	1.64	2.61	3.74	2.41	3.18	3.18	3.13	2.87	3.15
Gd	4.58	5.55	9.7	14.97	10.8	20.47	20.52	13.6	11.91	15.46
Tb	0.73	0.89	1.43	2.56	1.68	2.78	2.8	2.56	2.13	3.02
Dy	3.99	4.81	8.1	10.47	9.79	13.33	13.38	10.35	9.22	11.07
Er	2.41	2.69	4.26	6.62	5.59	9.72	9.75	6.45	5.68	7.46
Yb	2.11	2.45	3.96	5.62	5.24	6.73	6.75	5.36	4.78	5.56
Lu	0.33	0.39	0.58	1.18	0.71	0.9	0.98	0.87	0.77	0.94
Residue composition (%)										
Plagioclase An40								56.52	56.07	
Plagioclase An42						56.37	56.53			57.02
Clinopyroxene						17.56	17.4	18.84	18.87	16.99
Orthopyroxene						14.93	14.99	13.04	12.87	15.79
Ilmenite						2.65	2.63	2.9	3.19	2.27
Magnetite						8.5	8.45	8.7	9.01	7.93
r2						0.008	0.016	0.028	0.001	0.234
M-degree of melting						M = 8	M = 8	M = 29	M = 30	M = 17

1 — Partial melting (PM) — norite of Pium Complex to Planalto suite.
2 — Partial melting — quartz norite of Pium Complex to Planalto suite.
3 — Partial melting — norite to quartz gabbro of charnockitic association.
* Chemical composition from Santos (2009).
Co — Composition of the source.
HBSG — Hornblende–biotite syenogranite; BHMzG — Biotite–hornblende monzogranite; Qtz — Quartz.

by modeling. We devised FC models for the monzogranite–syenogranite lineage with AMR-209 (biotite–hornblende monzogranite) and AMR-208 (biotite syenogranite) as the initial and derived liquid, respectively. The models show a good fit for major elements and less conclusive or inconsistent for trace elements. This model was applied for the samples AMR-152 (biotite–hornblende monzogranite) and AMR-137 (biotite–hornblende syenogranite) of the type area of the Planalto granite with similar results. Major element fractional crystallization model indicates that a low degree of fractionation would be necessary to generate the more evolved liquids. This is consistent with the small difference in the degree of melting necessary to originate liquids of monzogranite and syenogranite composition from a more mafic protolith (Table 3). It is also noteworthy that the silica contents of monzogranites (70.39–74.86 wt.%) and syenogranites (71.66–75.51 wt.%) are largely superposed (Table 1). This evidence and the fact that there is no clear record of internal zoning in the plutons indicate that the monzogranites and syenogranites were more probably derived from small variations in the melting degree of the same sources and not by in situ fractional crystallization. These sources were probably geochemically similar to the mafic and intermediate rocks of the Pium complex.

6.1.2. Charnockitic rocks

The relationships between orthopyroxene-bearing mafic rocks similar in composition to the Pium complex rocks and the Neoarchean quartz gabbro were also examined. The orthopyroxene-bearing quartz gabbro (GRD-05) of the charnockitic association could possibly result to ~17% partial melting of the norite (sample CP-20, Table 3), leaving as residual phases the same minerals observed in the case of the Planalto granites. It is concluded that the quartz gabbros have chemical compositions compatible with their derivation from the Pium norite by partial melting processes. An alternative is that the charnockitic rocks were derived by fractional crystallization of a noritic magma, similar in composition to the Pium complex rocks but of younger age. In this case, a high degree of fractionation would be necessary.

It is concluded that the Neoarchean charnockitic rocks may have been derived by partial melting of a granulitic mafic crust similar in composition to the norite of the Pium complex. The similarity between the processes of origin of the Neoarchean charnockitic rocks and the Planalto suite granites implies a possible genetic link between them.

6.2. Planalto suite: A-type or hydrated charnockite rocks?

The Planalto suite and similar granites of the Carajás province have geochemical affinities with alkaline Archean granites and reduced-A-type granites and are ferroan. However, all these rocks are foliated, deformed, and interpreted as synkinematic granites, in the sense that they were strongly deformed during their

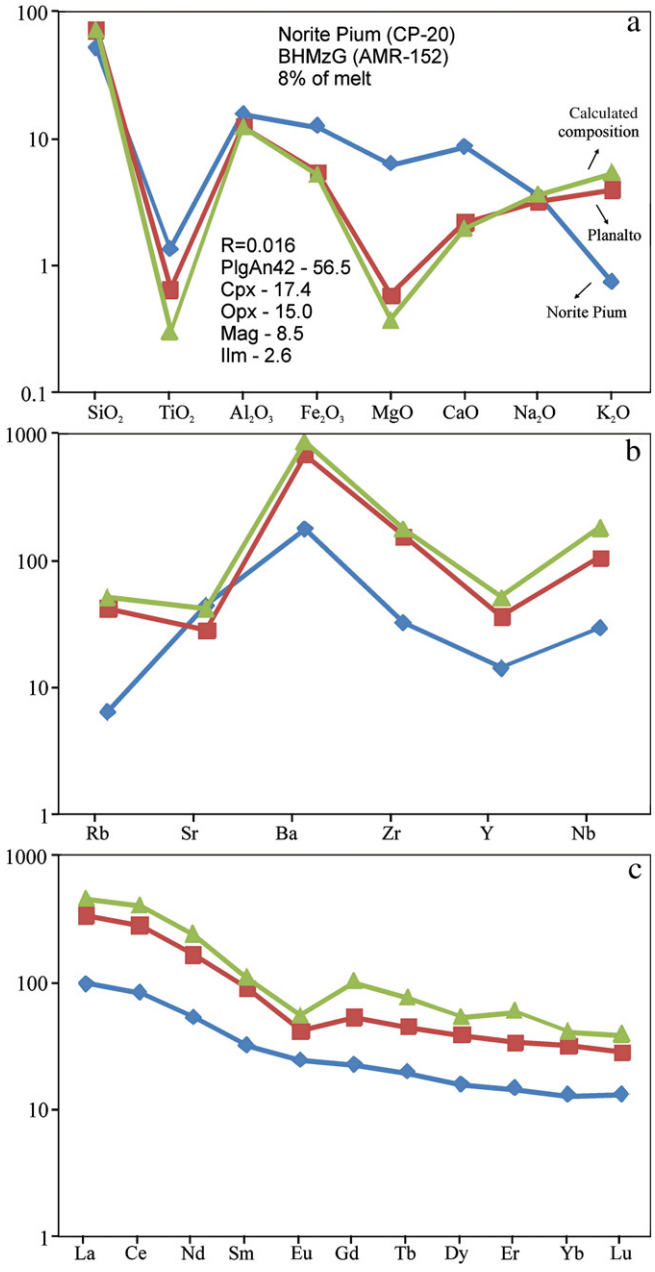

Fig. 11. Partial melting modeling of the Pium complex norite (CP-20) as a source of the Planalto granite magmas (AMR-152, hornblende–biotite monzogranite). (a) Major element modeling. (b) LILE and HFSE trace element modeling. (c) REE modeling.

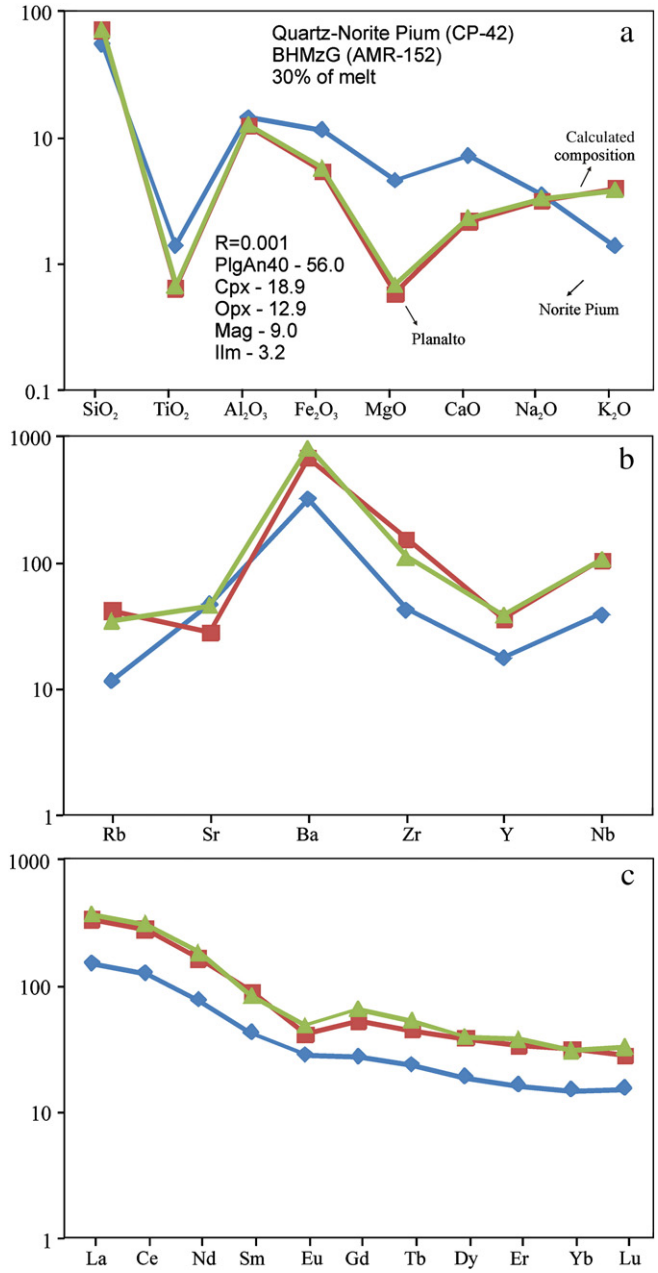

Fig. 12. Partial melting modeling of the Pium complex quartz norite (CP-42) as a source of the Planalto granite magmas (AMR-152, hornblende-biotite monzogranite). (a) Major element modeling. (b) LILE and HFSE trace element modeling. (c) REE modeling.

emplacement (Barros et al., 2009). In this respect they differ from classical A-type granites that are essentially related to extensional settings and generally little deformed. However, there are some examples of A-type-like granites with tholeiitic affinity that are syntectonic and deformed (Florisbal et al., 2009; Nardi and Bitencourt, 2009). On the other hand, the biotite–hornblende granites of the Planalto suite are closely associated with 'granulitic' and charnockitic rocks, and a granulitic source was admitted for the Estrela complex, Serra do Rabo and Igarapé Gelado plutons (Barros et al., 2009). A close relationship between orthopyroxene-bearing granitoids and biotite–hornblende granites was also noticed by Elliott (2003), who concluded that the Paleoproterozoic post-kinematic Jämsä and Honkajoki granitoids of the Central Finland Granitoid Complex have, respectively, C- and A-type geochemical affinities. According to Frost and Frost (2008, their Fig. 11), biotite–hornblende granites could be produced from hydrated, fluid-enriched residual melts of charnockite magma evolution. These residual melts will be formed at lower crustal levels compared to the associated charnockitic rocks, which could represent, at least in part, dry cumulates of the original magma. Mafic underplate, probably in an extensional tectonic setting, would be responsible for the melting of the crust and release of CO_2 and H_2O for higher levels. The general characteristics described in this particular geological setting are also shown by the Planalto and similar suites of the Carajás province with the difference that these are synkinematic granites possibly related to collision better than formed in an extensional setting (Barros et al., 2009).

The hydrated biotite–hornblende granitoids associated with charnockites can be ferroan or magnesian in character and related, respectively, to mafic underplate in extensional settings or to arc-related sources (Frost and Frost, 2008). It was also proposed that the term A-type granite should be replaced by ferroan granites (Frost and Frost, 2011). Accepting this broad definition, the Planalto suite and

similar granites of the Carajás province could be classified as A-type on the basis of their major and trace element signature including ferroan character (high HFSE and FeOt/(FeOt + MgO), low Al_2O_3 and CaO; Figs. 5 and 6). However, the structural features of the studied granites and their close association with charnockitic rocks are intriguing and denote a tectonic setting distinct of that generally admitted for A-type granites. This aspect and the large geochemical variation observed in the granitoids associated with charnockitic series could be seen as a restriction for the classification of their ferroan varieties as A-type granites. An alternative would be to classify the biotite–hornblende granites of the Planalto suite as hydrated granites of the charnockitic rocks series, independent of their FeOt/(FeOt + MgO) ratios.

It will be relevant to make further studies on hydrated biotite–hornblende granites associated with charnockitic series and similar geochemically to the A-type granites to achieve a better understanding of their geochemistry, origin, and classification. These granites are found in several cratons and are common in the Late Archean (Larin et al., 2006; Misra et al., 2002; Moore et al., 1993; Sheraton and Black, 1988). At the moment, we prefer classifying the studied granites of the Planalto suite as hydrated granites associated with charnockitic series. However, if a larger and more general definition of A-type or ferroan granites is adopted, they could also be classified as such. The only restriction to the classification of them as A-type granites is that it would imply formation of this kind of granite in synkinematic settings.

6.3. Tectonic significance of the Planalto Suite and similar granites

It is common to consider A-type granites to be associated with crustal extension in post-orogenic or anorogenic settings (Bonin, 2007; Collins et al., 1982; Dall'Agnol et al., 2005; Sylvester, 1989; Whalen et al., 1987). However, in the Carajás province, syntectonic or synkinematic Archean A-type granites contemporaneous with compressional stages are reported (Barros et al., 2009; Domingos, 2009). The emplacement model proposed for the Estrela complex in the Carajás basin involved recurrent injection of batches of magmas with the filling of the magma chamber promoting lateral expansion and flattening of the peripheral earlier pulses and adjacent country rocks (Barros et al., 2009). In the Canaã dos Carajás area of the Transition subdomain, a regional phase of sinistral transpression was accompanied by magmatism forming the E–W elongated, foliated A-type granites of the Planalto suite. Transpression produced a penetrative ductile fabric and most of the strain was accommodated in shear zones (Domingos, 2009). Araújo and Maia (1991) stated that the Pium complex and the granites now included in the Planalto suite correspond to deep crustal rocks transported along shear zones to comparatively shallower crustal levels.

Accepting that the Carajás basin was formed at ca. 2.76 Ga (the age of the metavolcanic rocks of the Itacaiúnas supergroup filling the basin; Gibbs et al., 1986; Machado et al., 1991) and was related to a in a continental tectonic setting, and considering the ages of the Estrela complex (2763 ± 7 Ma; Barros et al., 2009) and the Planalto suite (2747 ± 2 Ma, Huhn et al., 1999; 2754 ± 2 Ma, Silva et al., 2010; 2748 ± 2 Ma, 2749 ± 3 Ma, Souza et al., 2010), there is a problem to accommodate the extensional setting necessary for the development of the basin and the compressional setting implied in the syntectonic emplacement of the Estrela complex, Planalto suite and similar granites. In view of the ages above, the formation and filling of the basin are too close to the ages of the granites that evolved in a compressional setting. If correct, this would imply that the opening and inversion of the Carajás basin would be almost coincident in time. However, the age of ~2730 Ma obtained in this work for the crystallization and emplacement of the Planalto granite is significantly younger and more suitable for the inversion from an extensional to a compressional setting. Therefore, we can speculate that the Planalto suite magmas were formed by partial melting of mafic lower crustal rocks during a regional phase of sinistral transpression (Domingos, 2009). The resulting magmas initiated their crystallization at relatively deep crustal levels and were more probably largely crystallized during their emplacement in the upper crust. Their emplacement occurred under an active regional shear and associated with the major shear zones found in the Canaã dos Carajás area (Araújo and Maia, 1991; Domingos, 2009). This model explains the penetrative foliation and local stretching lineation observed in the Planalto granite.

On the other hand, the close association between the Planalto suite and the Pium complex and charnockitic rocks suggests a similarity between its evolution and that of the high temperature granite magmatism of the Mesoproterozoic Musgrave province of Central Australia (Smithies et al., 2011). In the Musgrave province there are widespread metaluminous and ferroan rocks ranging from alkali-calcic to calc-alkalic, with affinities with A-type granites and an orthopyroxene-bearing (charnockitic) primary mineralogy. Their evolution was attributed by Smithies et al. (2011) to MASH (melting, assimilation, storage, and homogenization) processes. The same model cannot be easily adapted for the Carajás region, because the evolution of the Musgrave province is apparently more complex as it was affected by 100 Myr long successive magmatic and metamorphic events at ultra-high temperature. This peculiar situation is possibly due to the fact that the Musgrave province is located in the join of three main older cratonic blocks and its evolution was related to mantle plume influence (Smithies et al., 2011). However, the Musgrave and Carajás provinces share the formation of charnockites and associated granites triggered by the underplating of mafic magmas at the base of the crust. Another aspect in common, and also registered in the Limpopo belt (Rapopo, 2010), is the generation of this kind of rock association near the limits between distinct tectonic blocks or in their zone of interaction (Smithies et al., 2011).

7. Conclusions

1. Our new LA-MC-ICPMS and Pb-evaporation geochronological data on zircon indicate that: (a) The orthopyroxene quartz gabbro associated with the Pium complex and Planalto suite has a crystallization age of 2735 ± 5 Ma; (b) The Pb-evaporation ages given by three samples of the Planalto suite are concentrated around 2730 Ma (2733 ± 2 Ma, 2731 ± 1 Ma and 2736 ± 4 Ma). The U–Pb LA-MC-ICPMS concordia ages obtained for the same samples are of 2729 ± 17 Ma, 2710 ± 10 Ma, and 2706 ± 5 Ma (the first of these superposed with those given by the Pb-evaporation method). An age of ~2730 Ma for the Planalto suite granites is also indicated by new U–Pb SHRIMP on zircon dating (Feio, 2011). Hence, the geochronological results indicate that the Planalto suite granites were crystallized at ca. 2730 ± 10 Ma, implying a little lower age than those available in the literature for similar granites of the Carajás province.
2. The Planalto suite granites are ferroan and similar geochemically to reduced A-type granites. Plagioclase was retained in the melting residue of the magma and garnet and hornblende where not important fractionating phases during the magma evolution. In previous works, these Archean granites and similar rocks of the Carajás province have been classified as A-type granites. However, the structural features of these units denote a syntectonic setting (uncommon for A-type granites). This aspect and the large geochemical variation observed in the granitoids associated with charnockite series keeps us from considering these ferroan granites as A-type granites and we regard them as hydrated granites of the charnockite series. The need for further studies on hydrated biotite–hornblende A-type like granites associated with the charnockite series is evident.
3. Geochemical modeling suggests that the Planalto suite could be derived by partial melting of mafic to intermediate tholeitic

orthopyroxene-bearing rocks similar to those of the Pium complex or, alternatively, by AFC processes involving a lower degree of assimilation of a mafic granulitic lower crust by a tholeiitic basalt magma that underwent a large extent fractional crystallization. The partial melting model is preferred. The dominant monzogranite and syenogranite varieties of the Planalto suite were derived from small variations in the melting degree of similar sources rather than by fractional crystallization.

4. Neoarchean charnockitic rocks associated with the Mesoarchean Pium complex have chemical compositions compatible with derivation from the Pium norite by partial melting (~17%).
5. At 2.76 Ga, upwelling of the asthenospheric mantle in an extensional setting propitiated the formation of the Carajás basin. Later on, at ca. 2.73 Ga, heat input from mafic magmas initiated partial melting of mafic to intermediate lower crustal rocks, originating the Planalto and charnockitic magmas. These magmas began to crystallize at relatively deep crustal levels and were largely crystallized during emplacement in the upper-middle crust. Their emplacement occurred under active regional stress and was associated with major shear zones found in the Canaã dos Carajás area. Moreover, the close association between the Planalto suite and charnockite rocks suggests similarity between its evolution and that of the high temperature granite magmatism commonly found near the border zones of tectonic blocks or in their zone of interaction.

Supplementary materials related to this article can be found online at doi:10.1016/j.lithos.2012.02.020.

Acknowledgments

F.J. Althoff, C.E.M. Barros, and A.A.S. Leite, are acknowledged for their support in geological mapping and J.E.B. Soares and M.A. Oliveira are acknowledged for previous work in the studied area. The authors thank: M.A. Galarza Toro for his assistance for obtainment of the single zircon Pb-evaporation analyses; M. Matteini, B. Lima, and J.A.C. Almeida for their assistance on LA-MC-ICPMS analyses; O.T. Rämö for previous discussions about geochronological data and petrogenesis and also for editorial work. C.N. Lamarão and I.M.O. Ramalho are also thanked for their assistance in the cathodoluminescence imaging. The reviews of Virginia McLemore and Lauro V.S. Nardi, helped to improve the original manuscript, and were complemented by helpful discussions with the latter. This research received financial support from CNPq (R. Dall'Agnol — Grants 0550739/2001-7, 476075/2003-3, 307469/2003-4, 484524/2007-0; PRONEX — Proc. 66.2103/1998-0; G.R.L Feio — CNPq scholarship), and Federal University of Pará (UFPA). This paper is a contribution to the IGCP 510 project (A-type Granites and Related Rocks through Time), to the Brazilian Institute of Amazonia Geosciences (INCT program –CNPq/MCT/FAPESPA – Proc. 573733/2008-2) and to the IGCP-SIDA 599 project (The Changing Early Earth).

Appendix A. Analytical procedures for whole-rock geochemical analyses

The chemical analyses for major elements and trace elements, including the REE, were performed by ICP-ES and ICP-MS, respectively, at the Acme Analytical Laboratories Ltd. in Canada.

Sm–Nd isotopic analyses followed the method described by Gioia and Pimentel (2000). They were performed at the Geochronology Laboratory of the University of Brasília. Whole rock powders (ca. 50 mg) were mixed with ^{149}Sm–^{150}Nd spike solution and dissolved in Savillex capsules. Sm and Nd extraction of whole rock samples followed conventional cation exchange techniques, using teflon columns containing LN-Spec resin (HDEHP–diethylhexyl phosphoric acid supported on PTFE powder). Sm and Nd samples were loaded on Re evaporation filaments of double filament assemblies and the isotopic measurements were carried out on a multi-collector Finnigan MAT 262 mass spectrometer in static mode. Uncertainties for Sm/Nd and $^{143}Nd/^{144}Nd$ ratios are better than ± 0.5% (2σ) and ± 0.005% (2σ), respectively, based on repeated analyses of international rock standards BHVO-1 and BCR-1 (BCR-1: $^{143}Nd/^{144}Nd = 0.512647 \pm 8$, Nd = 28.73 ppm and Sm = 6.66 ppm; BHVO-1: Nd = 24.83 ppm and Sm = 6.2 ppm). The $^{143}Nd/^{144}Nd$ ratios were normalized to $^{146}Nd/^{144}Nd$ of 0.7219 and the decay constant used was 6.54×10^{-12}. The TDM values were calculated using the model of DePaolo (1981).

Appendix B. Analytical methods of geochronology

Samples ARC-109, GRD-77, and AMR-187B (Planalto suite) and GRD-05 (orthopyroxene quartz gabbro) were selected for geochronological studies. All samples of the Planalto suite were analyzed by the Pb–Pb method and also by LA-MC-ICPMS. GRD-05 was analyzed only by LA-MC-ICPMS. Zircon concentrates were extracted from ca. 10 kg rock samples using conventional gravimetric methods of heavy mineral separation and magnetic (Frantz isodynamic separator) techniques at the Geochronology Laboratory of the University of Pará (Pará-Iso). Final purification was achieved by hand selecting through a binocular microscope and the zircon grains of each sample were then photographed under reflected light. For U–Pb LA-MC-ICPMS analyses, the zircons grains of each sample were mounted in epoxy resin, polished, and their internal structures were examined by cathodoluminescence (CL) imaging technique in a scanning electron microscope LEO 1430 at the Scanning Electron Microscopy Laboratory of the Geosciences Institute of Federal University of Pará (UFPA).

For the Pb-evaporation method (Kober, 1987), individual selected zircon grains were encapsulated in the Re-filament used for evaporation, which was placed directly in front of the ionization filament. The Pb is extracted by heating in three evaporation steps at temperatures of 1450º, 1500º, and 1550 °C and loaded on an ionization filament. The Pb intensities were measured by each peak stepping through the 206–207–208–206–207–204 mass sequence for five mass scans, defining one data block with eight $^{207}Pb/^{206}Pb$ ratios. The weighted $^{207}Pb/^{206}Pb$ mean for each block is corrected for common Pb using appropriate age values derived from the two-stage model of Stacey and Kramers (1975), and results with $^{204}Pb/^{206}Pb$ ratios higher than 0.0004 and those that scatter more than two standard deviations from the average age value were discarded. The calculated age for a single zircon grain and its error, according to Gaudette et al. (1998), is the weighted mean and standard error of the accepted blocks of data. The ages are presented with 2σ error.

The U–Pb LA-MC-ICPMS analyses were carried out using a New Wave UP213 Nd:YAG laser (λ — 213 nm), linked to a Thermo Finnigan Neptune multi-collector ICPMS at the Geochronology Laboratory of the University of Brasília. The analytical procedures were described by Buhn et al. (2009). The laser was run at a frequency of 10 Hz and energy of 0.4 mJ/pulse, ablation time of 40 s and a spot size of 30 μm in diameter. Plotting of U–Pb data was performed by ISOPLOT (Ludwig, 2001) and errors for isotopic ratios are presented at the 1σ level.

The analyses have been carried out using raster ablation method (Buhn et al., 2009) to prevent laser induced mass bias fractionation. The U–Pb raw data are translated to an Excel spreadsheet for data reduction and, when necessary, the laser induced mass bias was corrected using the method of Kosler et al. (2002). Common lead (^{204}Pb) interference and background correction, when necessary were carried out by monitoring the ^{202}Hg and 204 mass ($^{204}Hg + ^{204}Pb$) during the analytical sessions and using a model Pb composition (Stacey and Kramers, 1975) when necessary. Reported errors are propagated by quadratic addition $[(2SD^2 + 2SE^2)^{1/2}]$ of external reproducibility and within-run precision. The external reproducibility is represented by the standard deviation (SD) obtained by repeated

analyses (n = 20, ~0.8% for $^{207}Pb/^{206}Pb$ and ~1% for $^{206}Pb/^{238}U$) of standard zircon GJ-1, performed during analytical session, and the within-run precision is represented by the standard error (SE) that was calculated for each analysis.

For the exclusion of spot analyses on the calculation of U–Pb ages we have employed the general criteria adopted in the literature: (1) the common lead content (the $^{206}Pb/^{204}Pb$ ratio should not be lower than 1000); (2) the degree of discordance (not using data where the discordance is higher than 10%); (3) the analytical precision (not using the data where the isotopic ratios have error greater than 3%). These general criteria were refined for each specific sample.

Appendix C. Morphological aspects of the analyzed zircon crystals

Hornblende syenogranite (AMR-187B) — Zircon crystals are prismatic with slightly rounded edges, pale brown, translucent to transparent, and intensely fractured. Under cathodoluminescence (CL), two populations of zircon crystals (Fig. Aa; supplementary data) were distinguished: (1) Low-CL dark crystals that correspond to the more brownish grains; (2) bright crystals showing marked oscillatory zoning and sometimes gray shade cores and low-CL darker rims that locally form convolute zones in the crystals.

Hornblende–biotite syenogranite (ARC-109) — This sample has elongated, euhedral, prismatic, translucent to transparent pale pink zircons, and sparse inclusions and fractures. Under cathodoluminescence, the zircon crystals (Fig. Ab; supplementary data) show most commonly irregular and apparently corroded dark gray cores surrounded by larger outer zones with well developed oscillatory zoning and local dark rims similar to those seen in AMR-187B.

Biotite syenogranite (GRD-77) — the zircon crystals are colorless, transparent, prismatic and euhedral. CL images (Fig. Ac; supplementary data) show that the crystals are relatively more homogeneous than those of the other Planalto samples. They display strongly marked oscillatory zoning with local gray irregular cores and rare thin darker rims.

Orthopyroxene quartz gabbro (GRD-05) — Zircon crystals display commonly prismatic shape with well defined but rounded edges, light pink color and transparent. Cathodoluminescence images reveal the presence of gray cores surrounded by lighter outer zones with irregular oscillatory or convolute zoning (Fig. Ad; supplementary data).

References

Almeida, J.A.C., Dall'Agnol, R., Dias, S.B., Althoff, F.J., 2010. Origin of the Archean leucogranodiorite–granite suites: evidence from the Rio Maria terrane and implications for granite magmatism in the Archean. Lithos 120, 235–257.

Almeida, J.A.C., Dall'Agnol, R., Oliveira, M.A., Macambira, M.J.B., Pimentel, M.M., Rämö, O.T., Guimarães, F.V., Leite, A.A.S., 2011. Zircon geochronology and geochemistry of the TTG suites of the Rio Maria granite–greenstone terrane: implications for the growth of the Archean crust of Carajás Province, Brazil. Precambrian Research 120, 235–257.

Althoff, F.J., Barbey, P., Boullier, A.M., 2000. 2.8–3.0 Ga plutonism and deformation in the SE Amazonian craton: the Archean granitoids of Marajoara (Carajás Mineral province, Brazil). Precambrian Research 104, 187–206.

Anderson, J.L., Bender, B., 1989. Nature and origin of Proterozoic A-type granitic magmatism in the southwestern United States of America. Lithos 23, 19–52.

Araújo, O.J.B., Maia, R.G.N., 1991. Programa de levantamentos geológicos básicos do Brasil, Serra dos Carajás, folha SB-22-Z-A, Estado do Pará. Texto explicativo. DNPM/CPRM, Brasília. 164 pp. (in Portuguese).

Barros, C.E.M., Sardinha, A.S., Barbosa, J.P.O., Macambira, M.J.B., 2009. Structure, Petrology, Geochemistry and zircon U/Pb and Pb/Pb geochronology of the synkinematic Archean (2.7 Ga) A-type granites from the Carajás Metallogenic Province, northern Brazil. The Canadian Mineralogist 47, 1423–1440.

Bonin, B., 2007. A-type granites and related rocks: evolution of a concept, problems and prospects. Lithos 97, 1–29.

Buhn, B., Pimentel, M.M., Matteini, M., Dantas, E.L., 2009. High spatial resolution analysis of Pb and U isotopes for geochronology by laser ablation multi-collector inductively coupled plasma mass spectrometry (LA-MC-ICP-MS). Anais Academia Brasileira de Ciências 81, 1–16.

Champion, D.C., Sheraton, J.W., 1997. Geochemistry and Nd isotope systematics of Archean granites of the Eastern Goldfields, Yilgarn Craton, Australia: implications for crustal growth processes. Precambrian Research 83, 109–132.

Clemens, J.D., Holloway, J.R., White, A.J.R., 1986. Origin of the A-type granite: experimental constraints. American Mineralogist 71, 317–324.

Collins, W.J., Beams, S.D., White, A.J.R., Chappell, B.W., 1982. Nature and origin of A-type granites with particular reference to southeastern Australia. Contributions to Mineralogy and Petrology 80, 189–200.

Condie, K.C., 1993. Chemical composition and evolution of the upper continental crust: contrasting results from surface samples and shale. Chemical Geology 104, 1–37.

Dall'Agnol, R., Oliveira, D.C., 2007. Oxidized, magnetite-series, rapakivi-type granites of Carajás, Brazil: implications for classification and petrogenesis of A-type granites. Lithos 93, 215–233.

Dall'Agnol, R., Teixeira, N.P., Rämö, O.T., Moura, C.A.V., Macambira, M.J.B., Oliveira, D.C., 2005. Petrogenesis of the Paleoproterozoic, rapakivi, A-type granites of the Archean Carajás Metallogenic Province, Brazil. Lithos 80, 101–129.

Dall'Agnol, R., Oliveira, M.A., Almeida, J.A.C., Althoff, F.J., Leite, A.A.S., Oliveira, D.C., Barros, C.E.M., 2006. Archean and Paleoproterozoic granitoids of the Carajás Metallogenic Province, eastern Amazonian Craton. In: Dall'Agnol, R., Rosa-Costa, L.T., Klein, E.L. (Eds.), Symposium on Magmatism, Crustal Evolution, and Metallogenesis of the Amazonian Craton. : Abstracts Volume and Field Trip Guide. PRONEX-UFPA-SBGNO, Belém, pp. 99–150.

DePaolo, D.J., 1981. Neodymium isotope in the Colorado Front Range and crust–mantle evolution in the Proterozoic. Nature 291, 193–196.

Domingos, F.H., 2009. The structural setting of the Canaã dos Carajás region and Sossego-Sequeirinho deposits, Carajás — Brazil. University of Durham, England, 483 pp. (Ph.D. Thesis).

Eby, G.N., 1992. Chemical subdivision of the A-type granitoids: petrogenetic and tectonic implications. Geology 20, 641–644.

Elliott, B.A., 2003. Petrogenesis of the post-kinematic magmatism of the central Finland granitoid complex II; sources and magmatic evolution. Journal of Petrology 44, 1681–1701.

Emslie, R.F., 1991. Granitoids of rapakivi granite–anorthosite and related associations. Precambrian Research 51, 173–192.

Evensen, N.M., Hamilton, P.T., O'Nions, R.K., 1978. Rare earth abundances in chondritic meteorites. Geochimica et Cosmochimica Acta 39, 55–64.

Feio, G.R.L., 2011. Magmatismo granitóide arqueano da área de Canaã dos Carajás: Implicações para a evolução crustal da Província Carajás. Dr. Thesis, Programa de Pós-graduação em Geologia e Geoquímica, Universidade Federal do Pará, Belém, Brasil, 190 pp.

Florisbal, L.M., Bitencourt, M., Nardi, L.V., Conceição, R.V., 2009. Early post-collisional granitic and coeval mafic magmatism of medium- to high-K tholeiitic affinity within the Neoproterozoic southern Brasilian shear belt. Precambrian Research 175, 135–148.

Frost, C.D., Frost, B.R., 1997. Reduced rapakivi-type granites: the tholeiite connection. Geology 25, 647–650.

Frost, C.D., Frost, B.R., 2008. On charnockites. Gondwana Research 13, 30–44.

Frost, C.D., Frost, B.R., 2011. On ferroan (A-type) granitoids: their compositional variability and modes of origin. Journal of Petrology 32, 39–53.

Frost, B.R., Barnes, C., Collins, W., Arculus, R., Ellis, D., Frost, C., 2001. A chemical classification for granitic rocks. Journal of Petrology 42, 2033–2048.

Gabriel, E.O., Oliveira, D.C., Macambira, M.J.B., 2010. Caracterização geológica, petrográfica e geocronológica de ortopiroxênio-trondhjemitos (leucoenderbitos) da região de Vila Cedere III, Canaã dos Carajás-PA, Província Mineral de Carajás. SBG, Congresso Brasileiro de Geologia, 45. CDrom (in Portuguese).

Gaudette, H.E., Lafon, J.M., Macambira, M.J.B., Moura, C.A.V., Scheller, T., 1998. Comparison of single filament Pb-evaporation/ionization zircon ages with conventional U-/Pb results: examples from the Precambrian of Brazil. Journal of South American Earth Sciences 11, 351–363.

Gibbs, A.K., Wirth, K.R., Hirata, W.K., Olszewski Jr., W.J., 1986. Age and composition of the Grão Pará Group volcanics, Serra dos Carajás. Revista Brasileira de Geociências 16, 201–211.

Gioia, S.M.C.L., Pimentel, M.M., 2000. The Sm–Nd isotopic method in the Geochronology Laboratory of the University of Brasília. Anais da Academia Brasileira de Ciências 72, 219–246.

Gomes, A.C.B., Dall'Agnol, R., 2007. Nova associação tonalítica-trondhjemítica Neoarqueana na região de Canaã dos Carajás: TTG com altos conteúdos de Ti, Zr e Y. Revista Brasileira de Geociências 37, 182–193 (in Portuguese).

Huhn, S.B., Macambira, M.J.B., Dall'Agnol, R., 1999. Geologia e geocronologia Pb/Pb do granito alcalino arqueano Planalto, região da Serra do Rabo, Carajás-PA. Simpósio de Geologia da Amazônia, 6, pp. 463–466 (in Portuguese).

Kober, B., 1987. Single-grain evaporation combined with Pb+ emitter bedding for $^{207}Pb/^{206}Pb$ age investigations using thermal ion mass spectrometry, and implications to zirconology. Contributions to Mineralogy and Petrology 96, 63–71.

Kosler, J., Fonneland, H., Sylvester, P., Tubrett, M., Pedersen, R.B., 2002. U–Pb dating of detrital zircons for sediment provenance studies — a comparison of laser ablation ICPMS and SIMS techniques. Chemical Geology 182, 605–618.

Kretz, R., 1983. Symbols for rock-forming minerals. American Mineralogist 68, 277–279.

Landenberger, B., Collins, W.J., 1996. Derivation of A-type granites from a dehydrated charnockitic lower crust: evidence from the Chaelundi complex, eastern Australia. Journal of Petrology 37, 145–170.

Larin, A.M., Kotov, A.B., Sal'nikova, E.B., Glebovitskii, V.A., Sukhanov, M.K., Yakovleva, S.Z., Kovach, V.P., Berezhnaya, N.G., Velikoslavinskii, S.D., Tolkachev, M.D., 2006. The Kalar Complex, Aldan–Stanovoi Shield, an ancient anorthosite–mangerite–charnockite–granite association: geochronologic, geochemical, and isotopic–geochemical characteristics. Petrology 14, 2–20.

Lauri, L.S., Rämö, O.T., Huhma, H., Mänttäri, I., Räsänen, J., 2006. Petrogenesis of silicic magmatism related to the 2.44 Ga rifting of Archean crust in Koillismaa, eastern Finland. Lithos 86, 137–166.

Le Maitre, R.W., Streckeisen, A., Zanettin, B., Le Bas, M.J., Bonin, B., Bateman, P., Bellieni, G., Dudek, A., Efremova, J., Keller, J., Lameyre, J., Sabine, P.A., Schmidt, R., Sørensen, H., Woolley, A.R., 2002. Igneous rocks. A classification and glossary of terms. Recommendations of the International Union of Geological Sciences Subcommission on the Systematics of Igneous Rocks. Cambridge University Press, Cambridge. 236 pp.

Leite, A.A.S., Dall'Agnol, R., Macambira, M.J.B., Althoff, F.J., 2004. Geologia e Geocronologia dos granitóides Arqueanos da região de Xinguara (PA) e suas implicações na evolução do Terreno Granito-Greenstone de Rio Maria. Revista Brasileira de Geociências 34, 447–458 (in Portuguese).

Lobato, L.M., Rosière, C.A., Silva, R.C.F., Zucchetti, M., Baars, F.J., Sedane, J.C.S., Javier Rios, F., Pimentel, M., Mendes, G.E., Monteiro, A.M., 2006. A mineralização hidrotermal de ferro da Província Mineral de Carajás — controle estrutural e contexto na evolução metalogenética da província. In: Marini, O.J., Queiroz, E.T., Ramos, B.W. (Eds.), Caracterização de Depósitos Minerais em Distritos Mineiros da Amazônia, DNPM, CT-Mineral/FINEP, ADIMB, pp. 25–92.

Loiselle, M.C., Wones, D.R., 1979. Characteristics and origin of anorogenic granites. Geological Society of America, Abstract, 11, p. 468.

Ludwig, K.R., 2001. User's manual for Isoplot/Ex Version 2.49 A geochronological toolkit for Microsoft Excel. Berkeley Geochronological Center Special Publication 1, 1–55.

Macambira, M.J.B. 1992. Chronologie U/Pb, Rb/Sr, K/Ar et croissance de la croûte continentale dans L'Amazonie du sud-est; exemple de la région de Rio Maria, Province de Carajas, Brésil. Université Montpellier II — France. 212 pp. (Ph.D. thesis; in French).

Macambira, J.B., 2003. O ambiente deposicional da Formação Carajás e uma proposta de modelo evolutivo para a Bacia Grão Pará. Universidade de Campinas — São Paulo. 217 pp. (Ph.D. thesis; in Portuguese).

Macambira, M.J.B., Lancelot, J., 1996. Time constraints for the formation of the Archean Rio Maria crust, southeastern Amazonian Craton, Brazil. International Geology Review 38, 1134–1142.

Machado, N., Lindenmayer, Z.G., Krogh, T.E., Lindenmayer, D., 1991. U–Pb geochronology of Archean magmatism and basement reactivation in the Carajás area, Amazon shield, Brazil. Precambrian Research 49, 329–354.

Misra, S., Sarkar, S.S., Ghosh, S., 2002. Evolution of Mayurbhanj granite pluton, eastern Singhbhum, India: a case study of petrogenesis of an A-type granite in bimodal association. Journal of Asian Earth Sciences 20, 965–989.

Moore, M., Davis, D.W., Robb, L.J., Jacson, M.C., Globler, D.F., 1993. Archean rapakivi granite–anorthosite–ryolite complex in the Witwatersrand basin hinterland, Southern Africa. Geology 21, 1031–1034.

Moreto, C.P.N., Monteiro, L.V.S., Xavier, R.P., Amaral, W.S., Santos, T.J.S., Juliani, C., Souza Filho, C.R., 2011. Mesoarchean (3.0 and 2.86 Ga) host rocks of the iron oxide–Cu–Au Bacaba deposit, Carajás Mineral Province: U–Pb geochronology and metallogenetic implications. Mineralium Deposita 46, 789–811.

Nardi, L.V.S., Bitencourt, M.F., 2009. A-type granitoids in post-collisional settings from southernmost Brazil: their classification and relationship with magmatic series. The Canadian Mineralogist 47, 1493–1504.

Nogueira, A.C.R., Truckenbrodt, W., Pinheiro, R.V.L., 1995. Formação Águas Claras, Pré-Cambriano da Serra dos Carajás: redescrição e redefinição litoestratigráfica. Boletim Museu Paraense Emílio Goeldi 7, 177–277 (in Portuguese).

Oliveira, M.A., Dall'Agnol, R., Althoff, F.J., Leite, A.A.S., 2009. Mesoarchean sanukitoid rocks of the Rio Maria Granite–Greenstone Terrane, Amazonian craton, Brazil. Journal of South American Earth Sciences 27, 146–160.

Patiño Douce, A.E., 1997. Generation of metaluminous A-type granites by low-pressure melting of calc-alkaline granitoids. Geology 25, 743–746.

Pidgeon, R.T., Macambira, M.J.B., Lafon, J.M., 2000. Th–U–Pb isotopic systems and internal structures of complex zircons from an enderbite from the Pium Complex, Carajás Province, Brazil: evidence for the ages of granulites facies metamorphism and the protolith of the enderbite. Chemical Geology 166, 159–171.

Rämö, O.T., Haapala, I., 1995. One hundred years of rapakivi granite. Mineralogy and Petrology 52, 129–185.

Rämö, O.T., Haapala, I., 2005. Rapakivi granites. In: Lehtinen, M., Nurmi, P.A., Rämö, O.T. (Eds.), Precambrian Geology of Finland — Key to the Evolution of the Fennoscandian Shield. Elsevier, Amsterdam, pp. 533–562.

Rämö, O.T., Vaasjoki, M., Mänttäri, I., Elliott, B.A., Nironen, M., 2001. Petrogenesis of the post-kinematic magmatism of the central Finland granitoid complex I; radiogenic isotope constraints and implications for crustal evolution. Journal of Petrology 42, 1971–1993.

Rapopo, M., 2010. Petrogenesis of the Matok pluton, South Africa: implications on the heat source that induced regional metamorphism in the Southern Marginal Zone of the Limpopo Belt. University of Stellenbosch, South Africa, 117 pp. (Master thesis).

Ricci, P.S.F., Carvalho, M.A., 2006. Rocks of the Pium-Area, Carajás Block, Brazil — a deep seated high-T gabbroic pluton (charnockitoid-like) with xenoliths of enderbitic gneisses dated at 3002 Ma — the basement problem revisited. Simpósio de Geologia da Amazônia, 8. CDroom (in Portuguese).

Rollinson, H.R., 1993. Using Geochemical Data: Evaluation, Presentation, and Interpretation. Longman, New York. 352 pp.

Santos, R.D., 2009. Geologia, petrografia e caracterização geoquímica das rochas máficas (granulitos?) do Complexo Pium – regiões de Vila Feitosa e Cedere III, Canaã dos Carajás – Província mineral de Carajás. Trabalho de conclusão de curso. Universidade Federal do Pará. 73 pp. (in Portuguese).

Santos, R.D., Oliveira, D.C., 2010. Geologia, petrografia e caracterização geoquímica das rochas máficas do Complexo Pium — Província Mineral de Carajás. Congresso Brasileiro de Geologia, 45. CDrom (in Portuguese).

Santos, J.O.S., Hartmann, L.A., Gaudette, H.E., Groves, D.I., McNaughton, N.J., Fletcher, I.R., 2000. A new understanding of the provinces of the Amazon Craton based on integration of field mapping and U–Pb and Sm–Nd geochronology. Gondwana Research 3, 453–488.

Sardinha, A.S., Dall'Agnol, R., Gomes, A.C.B., Macambira, M.J.B., Galarza, M.A., 2004. Geocronologia Pb–Pb e U–Pb em zircão de granitóides arqueanos da região de Canaã dos Carajás, Província Mineral de Carajás. Congresso Brasileiro de Geologia, 42. CDrom (in Portuguese).

Sardinha, A.S., Barros, C.E.M., Krymsky, R., 2006. Geology, Geochemistry, and U–Pb geochronology of the Archean (2.74 Ga) Serra do Rabo granite stocks, Carajás Province, northern Brazil. Journal of South American Earth Sciences 20, 327–339.

Shand, S.J., 1950. Eruptive rocks, 4th ed. Murby, London. (1950).

Sheraton, J.W., Black, L.P., 1988. Chemical evolution of granitic rocks in the East Antarctic Shield, with particular reference to post-orogenic granites. Lithos 21, 37–52.

Silva, M.L.T., Oliveira, D.C., Macambira, M.J.B., 2010. Geologia, petrografia e geocronologia do magmatismo de alto K da região de vila Jussara, Água Azul do Norte — Província Mineral de Carajás. Congresso Brasileiro de Geologia, 45. CDrom (in Portuguese).

Smithies, R.H., Howard, H.M., Evins, P.M., Kirkland, C.L., Kelsey, D.E., Hand, M., Wingate, M.T.D., Collins, A.S., Belousova, E., 2011. High-temperature granite magmatism, crust–mantle interaction and the mesoproterozoic intracontinental evolution of the Musgrave Province, Central Australia. Journal of Petrology 52, 931–958.

Souza, Z.S., Potrel, A., Lafon, J.M., Althoff, F.J., Pimentel, M.M., Dall'Agnol, R., Oliveira, C.G., 2001. Nd, Pb and Sr isotopes in the Identidade Belt, an Archean greenstone belt of Rio Maria region (Carajás Province, Brazil): implications for the geodynamic evolution of the Amazonian Craton. Precambrian Research 109, 293–315.

Souza, M.C., Oliveira, D.C., Macambira, M.J.B., Galarza, M.A., 2010. Geologia, petrografia e geocronologia do granito de alto K da região de Velha Canadá, município de Água Azul do Norte — Província Mineral de Carajás. Congresso Brasileiro de Geologia, 45. CDrom (in Portuguese).

Stacey, J.S., Kramers, J.D., 1975. Approximation of terrestrial lead isotope evolution by a two stage model. Earth and Planetary Science Letters 26, 207–221.

Sylvester, P.J., 1989. Post-collisional alkaline granites. Journal of Geology 97, 261–280.

Sylvester, P.J., 1994. Archaean granite plutons. In: Condie, K. (Ed.), Archean Crustal Evolution. Elsevier, Amsterdam, pp. 261–314.

Tassinari, C.C.G., Macambira, M., 2004. A evolução tectônica do Craton Amazônico. In: Mantesso-Neto, V., Bartorelli, A., Carneiro, C.D.R., Brito Neves, B.B. (Eds.), Geologia do Continente Sul Americano: Evolução da obra de Fernando Flávio Marques Almeida, pp. 471–486. São Paulo: BECA (in Portuguese).

Teixeira, L.R., 2005. Genesis versão 4.0. Aplicativo de modelamento geoquímico. Universidade Federal da Bahia. (in Portuguese).

Teixeira, J.B.G., Eggler, D.H., 1994. Petrology, geochemistry, and tectonic setting of Archean basaltic and dioritic rocks from the N4 iron deposit, Serra dos Carajás, Pará, Brazil. Acta Geology Leopoldensia 17, 71–114.

Vasquez, L.V., Rosa-Costa, L.R., Silva, C.G., Ricci, P.F., Barbosa, J.O., Klein, E.L., Lopes, E.S., Macambira, E.B., Chaves, C.L., Carvalho, J.M., Oliveira, J.G., Anjos, G.C., Silva, H.R., 2008. Geologia e Recursos Minerais do Estado do Pará: Sistema de Informações Geográficas — SIG: texto explicativo dos mapas Geológico e Tectônico e de Recursos Minerais do Estado do Pará. 328 pp. (in Portuguese).

Whalen, J.B., Currie, K.L., Chappell, B.W., 1987. A-types granites: geochemical characteristics, discrimination and petrogenesis. Contributions to Mineralogy and Petrology 95, 407–419.